

2.1 General Background

The Space Age began in 1957, with an 83 kg Russian Sputnik satellite bleeping greetings to a surprised world. Since that spectacular beginning, intensive effort has gone into the scientific exploration of space, exploration of the Moon and distant planets, manufacturing of materials in space laboratories, and exploiting orbiting satellites for communication, navigation and observation of the Earth. The early steps have passed into history, and most equipment and instrumentation has been and will continue to be replaced by lighter and more complex substitutes. The remarkable achievements of the Apollo Lunar Exploration Programme two decades ago still tend to overshadow the unmanned automated satellite flights, and it is not always realized that spacecraft orbiting above all continents of the world have already revolutionized global communications, maritime navigation, and worldwide weather forecasting. These satellites are now vital links in a global network. They would not have been economically or technically feasible before the advent of near-Earth space explorations.

Satellite communications started on a commercial basis with the launch of Early Bird in 1965, less than eight years after the launch of the first Sputnik. This was the first satellite to remain stationary over the Earth, and it was able to provide a continuous connection between any two Earth stations. Until comparatively recently these so-called ‘applications’ satellites were merely assemblies of separately designed components rather than thoughtfully integrated systems. Often component interfaces failed to match, reducing the overall system performance.

These satellites, and to a more limited extent the ‘scientific’ satellites, are now incorporating standardized subsystems in an attempt to optimize performance factors including weight, reliability, and cost.

It seems likely that the spacecraft designer has placed greatest emphasis on mass, as this is usually set by the

capabilities of the assigned launch vehicle which will take the satellite from the Earth’s surface and inject it into the desired orbit. The lighter the satellite, the cheaper will be the launch costs. Another major performance factor, reliability, can also be purchased if money is preferentially funneled into reliability and test programmes rather than launch vehicles. The important point is that performance factors of weight, reliability, and cost are all interrelated. The designer of an applications satellite will be more willing to pay for the reliability level that would give him 10 years of operation than the designer of a scientific satellite designed to shut off transmission after only one year when the mission objectives are attained.

One of the major aims of the European satellite manufacturer has been to set up a European communications programme which will develop and launch long-life satellites. A supporting technology programme has been undertaken to develop and qualify most of the critical subsystems that will enter the design of future operational satellites. An experimental satellite (Orbital Test Satellite—OTS) was launched in 1978 to evaluate and test the performance of the various subsystems of future European communication satellite systems. OTS and its launcher are illustrated in Figs. 2.1a and 2.2. Its major subsystems under evaluation included:

- *communications*—to relay information (data and commands) between Earth and satellite and, in concept, to and from other spacecraft.
- *power supply*—to provide electrical power to all satellite subsystems.
- *on-board propulsion*—to provide thrust for orbit changes, station-keeping, and deorbiting.
- *Environmental control*—to maintain specified temperatures, radiation levels, electromagnetic environment, etc.
- *structure*—to support and maintain satellite configuration on the ground, during launch and in orbit.

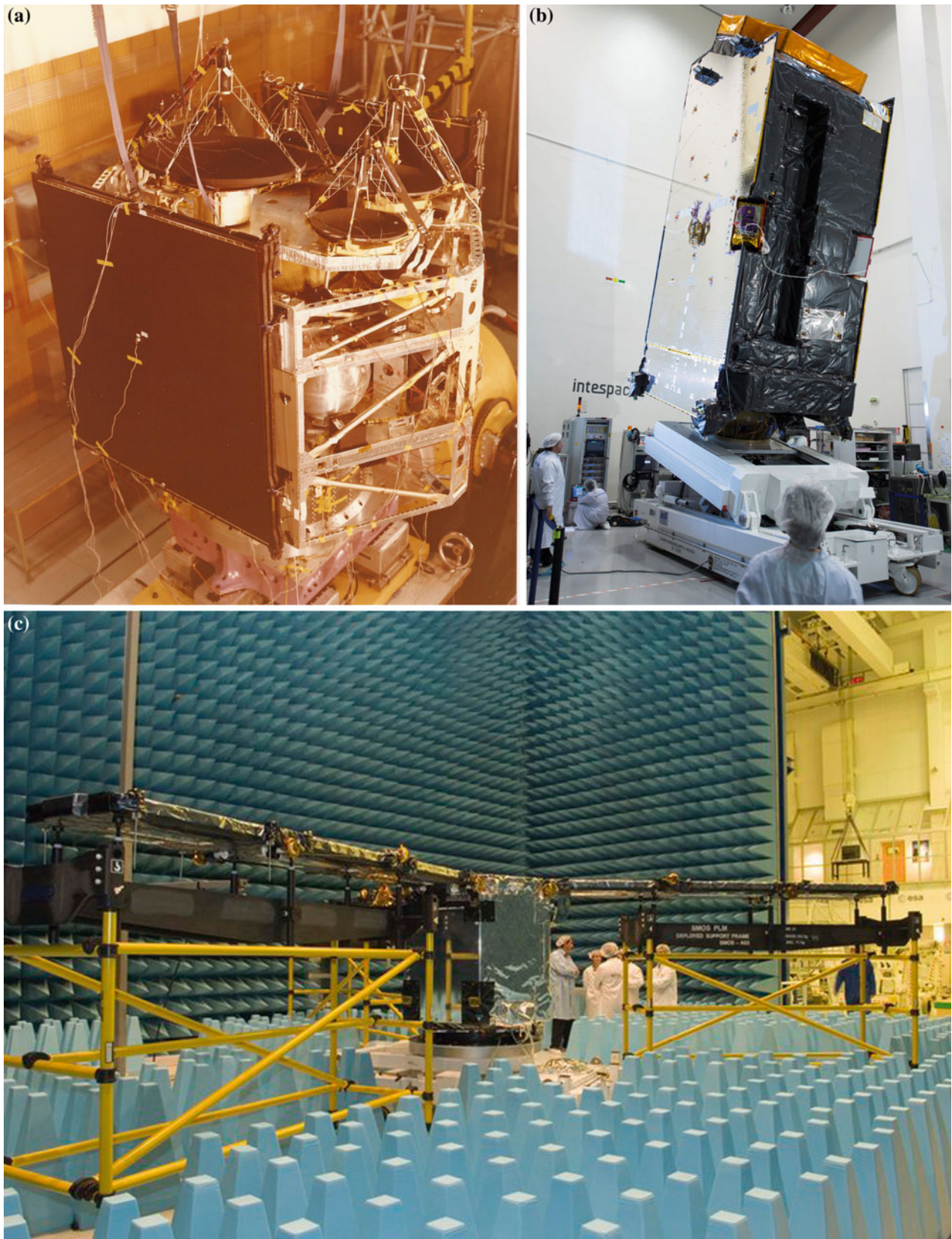
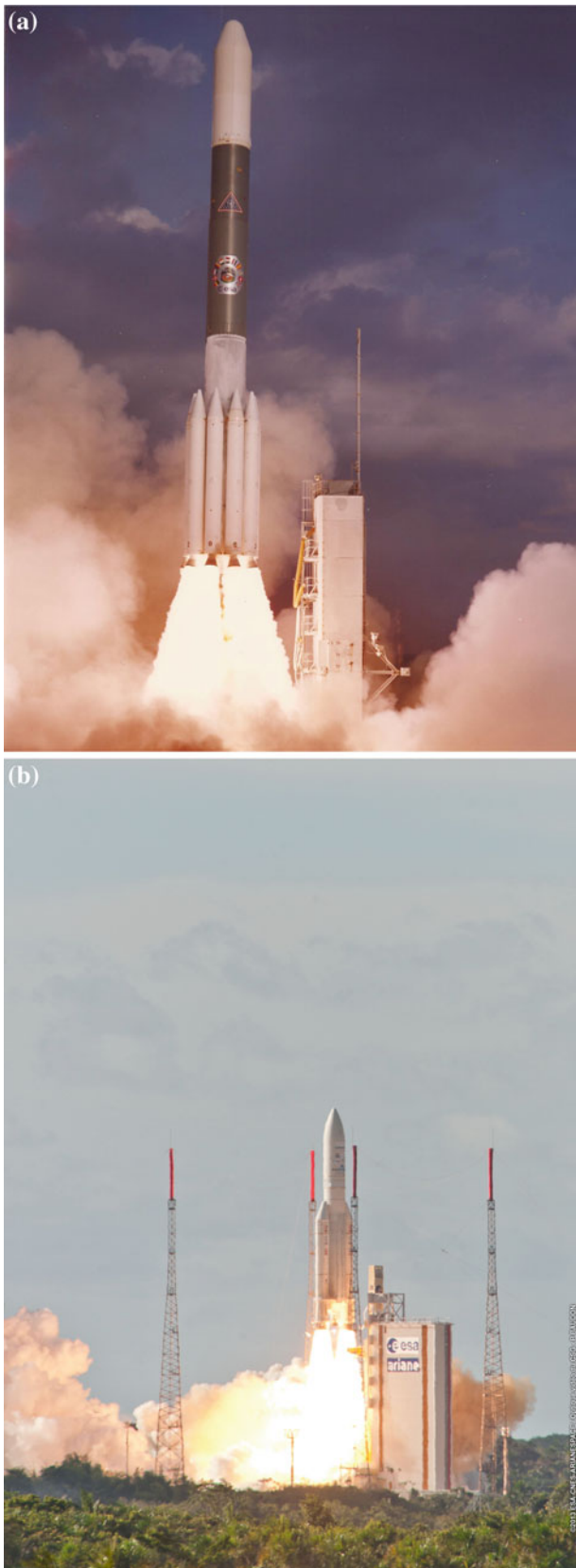


Fig. 2.1 **a** OTS 'structural model' during vibration testing in 1975. Thermal blankets are not yet fitted. This is the first ESA communication satellite and has a height of 2.5 m (ESA). **b** View of the Alphasat satellite, after tests in the Intespace's anechoic test chamber, Toulouse,

France, 15 March 2013. This communications satellite is 7.1 m high (ESA). **c** These 9 m-high spike-lined walls enclose the hushed interior of ESA's Maxwell test chamber, which isolates satellites from all external influences to assess their electromagnetic compatibility (ESA)



◀ **Fig. 2.2** **a** Launch of the European orbital test satellite (OTS-2, in 1978) on a Thor Delta rocket at Cape Canaveral. The 2 TV channels and 5000 telephone circuits operated without defects between 52 ground-stations (between Norway and Egypt) (ESA). **b** Launch of Alphasat—on the 25th July 2013, an Ariane 5 lifted off Europe’s largest telecommunications satellite (ESA)

The general development plan for a new satellite type such as OTS involves the building of several test models such as a structural model, thermal model, and engineering model (refurbished from the thermal model), before constructing the qualification model and finally a flight spacecraft.

Alphasat, shown in Fig. 2.1b is a high-power telecom satellite built by Astrium, through a public–private partnership between ESA and UK operator Inmarsat. It is based on the mighty Alphabus, the new European telecom platform developed by Astrium and Thales Alenia Space under joint contract from ESA and the French space agency, CNES. Alphabus is Europe’s response to increased market pressure for larger telecom payloads for direct-to-home TV broadcasting, digital audio broadcasting, broadband access and mobile services. Alphabus incorporates innovative technologies including:

- *electric propulsion*—to optimise the satellite’s mass in favour of payload
- *modular payload*—including an antenna module which can be adapted for different missions
- *star trackers*—ensure highly accurate attitude and orbit control
- *lithium ion cell batteries*—charged from high-performance solar cells

Whereas OTS generated 1260 W from its pair of solar panels, feeding to two 24 Ah NiCd batteries and had a weight of only 1490 kg, Alphasat can accommodate missions with up to 18 kW of payload power and has a weight of 6000 kg.

Organisations such as the EU, ESA and NASA use measures to assess the maturity of evolving technologies which can be related to devices, materials, components, etc. Regarding materials, mechanical parts and manufacturing processes, a new breakthrough or invention will not be suitable for immediate use and some basic research will have to be conducted. This may lead to the technology being assessed for feasibility, for development and later the technology may be demonstrated in a laboratory environment. Validation of the new material may be made according to certain test methods. Mechanical parts may be qualified and manufacturing processes may be verified by the testing of “technology

samples”—these are the steps usually taken in order to get approvals for space use by authorities (ECSS-Q-STD-70 2014). As a guide, the following listing can be used to assess the level of readiness of any materials technology:

Technology Readiness Level	Description
TRL 1	Basic principles observed and reported
TRL 2	Technology concept and/or application formulated
TRL 3	Analytical and experimental critical function and/or characteristic proof-of-concept
TRL 4	Component and/or breadboard validation in laboratory environment
TRL 5	Component and/or breadboard validation in relevant environment
TRL 6	System/subsystem model or prototype demonstration in a relevant environment (ground or space)
TRL 7	System prototype demonstration in a space environment
TRL 8	Actual system completed and “Flight qualified” through test and demonstration (ground or space)
TRL 9	Actual system “Flight proven” through successful mission operations

The reader may consider the above Technology Readiness Levels (TRLs) during the selection of materials and processes for a new application intended for use on board a spacecraft or even during the construction of a ground station (launch site). Obviously for any technology: the lower the TRL the more time and effort will be required before the approving authority can give authorisation for its incorporation into a space system. The concept of TRL’s will not be addressed during the following chapters of this book as every approval of a space material, mechanism and process will depend on the very precise requirements of a given space project. For some projects there may be an accepted higher level of risk involved during the selection of technologies. Low budget space flight experiments, providing they do not constitute a risk to the overall project, might choose to fly breadboard models that can give sufficient data return to university

projects. At the other end of the spectrum, manned flight safety management will differentiate between “systems safety” and “payload safety”. Space systems safety will be a trade-off between complex project elements using flight proven technologies—here astronaut safety must be of paramount importance. Payload safety will consider the materials, mechanical parts and manufacturing processes and whether the payload is essential for flight operations and crew safety. Payloads and experiments can fail and not cause a risk to the astronauts. However, the materials from which they are manufactured will be of particular concern as these may operate beyond their intended temperatures; it is essential that these, usually non-metallic materials, do not release toxic substances by off-gassing, nor any fire hazard because of the flammable nature of the piece-part.

2.2 Considerations for Materials and Processes

2.2.1 General Considerations During the Selection of Materials and Processes

The change of emphasis in Europe from building scientific satellites during the 1970’s with designed mission lives of one or two years to the production of a new generation of application satellites, which must be assured for periods of greater than twenty years in a somewhat hostile space environment, has necessitated that a greater effort is placed on confirming the reliability of many materials and technologies which have previously been accepted as virtually fault-free. Additionally, the new modular approach and the drive to standardize subsystems for easy and economical adaptation for different satellite missions has led to long ground storage periods. This can cause material degradation problems, particularly the decay of liquid and solid fuels and the general corrosion of sensitive surfaces and even stress corrosion of structural elements. A listing of materials approved and utilized for the fabrication of a satellite such as the aforementioned Orbital Test Satellite in 1975 included at least 500 different organic and inorganic materials. Each was preliminarily approved for use in a given application, bearing in mind the environmental conditions it has been designed to withstand. The Declared Materials Lists associated with multipurpose space platforms for large telecommunications payloads, such as the 6.6 t Alphasat launched in 2013, involve more than 1000 different materials. Until the late 1980s metallic materials have been the basic building materials of all satellites and launch vehicles with only a limited number of inroads from carbon fibre

reinforced plastics (CFRP). Because of their exact alignment requirements some solar panels, dish antennas, and antenna platforms are fabricated from CFRP which, because of its small coefficient of expansion, will retain dimensional accuracy under the changing temperature conditions of an orbit (-160 to $+180$ °C). Launch vehicles, satellites, space probes and manned modules are predominantly built by industrial concerns engaged in aircraft manufacture (e.g. “prime contractors” such as Boeing, Airbus, Lockheed Martin, Alenia, Aerospaziale and Astrium). Because of this, designers will prefer to choose structural and mechanical parts from traditional metal alloys and composites, and will limit manufacturing to joining and finishing technologies which already exist in their respective plants. When compared to a mass production industry there is often little incentive to promote the use of advanced materials and alloys which may improve reliability and be weight-saving but will suffer the drawback of requiring costly fundamental testing and qualification before being incorporated into space hardware.

Discussions between customers, prime contractors and their sub-tier suppliers involve contract requirement negotiations related to Materials and Processes issues and a considerable number of reviews will take into account such topics as design, materials selection, and fabrication processes. These are held throughout the various stages of every space project, from inception on the drawing board until the environmental testing and qualification of manufactured hardware prior to launch. However, it is not until the actual hardware is seen that one is struck by the results of cooperation between the many engineering disciplines. It is probable that the introduction of *computer-aided design* now means that spacecraft subassemblies and piece-parts are being fabricated to the closest tolerances ever achieved. The optimization of structural weight and the smaller design margins mean that a thorough knowledge of the materials selected for the application must be well established. This is particularly true for new, advanced materials, as the small design margins means there is no longer a reserve of strength built into the structure, as was the case for earlier spacecraft, to cover ignorance of design loads or stress intensities. The safety margins required of materials are real, but the over-conservative designs originating from so-called ‘gloom factors’ or scatter in materials properties should be a thing of the past.

To illustrate the accuracy demanded of modern machining capabilities one can consider the unfortunate situation of the flawed primary mirror of the Hubble Space Telescope (HST). The prime objective of the HST mission was to obtain images of astronomical objects in approximately ten times sharper detail than that obtained by ground-based telescopes. The HST 2.4 m mirror was designed to be a precisely calculated hyperboloid. Although the mirror is actually smooth to a precision of $1/64$ the wavelength of

light (or one-millionth of an inch), a calculation error caused the mirror which was originally launched to have been fabricated with a curvature that was too shallow with a total centre-to-edge error of about $2\text{ }\mu\text{m}$ (or $1/50$ thickness of a human hair). The result was that light rays hitting the mirror edges eventually made focus to a point that was slightly away from where light rays from the centre of the mirror focused: a defect called spherical aberration. The HST, delayed three years by the *Challenger* disaster, was launched in April 1990. Despite the flawed mirror, which rendered many of Hubble’s initial observations fuzzy, the new spaceborne telescope quickly demonstrated the advantages of an orbiting platform free from the interference of the Earth’s atmosphere. After the dramatic December 1993 repair mission, using astronauts from Space Shuttle *Endeavour* to correct the mirror and solar panel (see Sect. 8.2) problems, Hubble began to demonstrate its full potential to peer into the universe.

2.2.2 Some Futuristic Ideas

Advanced materials are finding more and more applications in new designs, and this is particularly true of reinforced polymers based on carbon or Kevlar fibres, clean materials (with low outgassing), and several new types of lightweight metal alloys. The microminiature electronic circuits so important for the relay of enormous volumes of data within a fraction of a second are also incorporating new materials with unique physical characteristics. Microdevices continue to be designed and prototyped (David 1996)—today these are termed micro-electro-mechanical systems (MEMS). Although many MEMS devices have been manufactured, to date, the only devices that have flown are accelerometers and gyroscopes (de Rooij 2009). In the USA, the JPL Centre for Space Microelectronics Technology has already produced a micro seismometer having a diameter of 12 mm and a ‘camera on a chip’ about the size of a fingernail. These kinds of advancement will certainly lead to smaller, lighter, and less costly spacecraft for the future. Even the so-called ‘nano satellite’, weighing about 1–2 kg, is thought to be feasible due to breakthroughs in small-scale engineering of MEMS. The cost of launching a satellite into LEO by the Space Shuttle was about £14,000 per kilogram and now, £5000 to £12,000 per kilogram when an ELV is selected. Costs to place a spacecraft into a geosynchronous transfer orbit (GTO) are estimated to be between and £20,000 per kilogram. Either launch vehicles should become less expensive, or satellites need redesigning to become far smaller and lighter so that multiple payloads (or even nanosats) can be launched simultaneously. A proliferation in the number of miniaturised satellites (often referred to as CubeSats) have been built by companies such as Clyde Space and SSTL

(now part of Airbus) but probably the majority of those presently in orbit originate from schools and universities. These have low construction costs combined with fewer materials and processes requirements. Many have applications beyond those of academic research or technology demonstration, and are used for Earth observation and defense purposes.

The future will see more advanced manufacturing processes involved with the construction of space hardware—even traditional methods such as casting and forging will probably be to closer specification and under more highly inert atmospheres. The autoclave curing of composites will be done under clean conditions without the use of low volatile organic materials and any mold release agents will not contain silicones as they are difficult to remove prior to painting. Friction stir welding and FricRiveting can be envisaged for joining metals to thermoplastics; and laser materials processing will involve localized, intense heating of solid targets and components by laser, to achieve ultrafast, novel and economic joining and surface engineering.

It used to be impossible to select a material without a full knowledge of how it might best be processed into a final piece-part—but today it seems that 3D printing has opened up a world of endless possibilities for designing and creating everything from a complex space mechanism to printed chocolates and foods for astronauts! 3D printing, also known as additive manufacturing (AM), produces three-dimensional items by “printing” them, layer-by-layer from raw ingredients consisting of powdered plastics, aluminium alloys, titanium alloys, low expansion alloys and other spacecraft materials. The most usual processing method is to introduce metal powder into a laser beam—a precise deposition of either sintered or melted powder is directed onto a flat table. The laser beam is controlled by CAD programs to raster across the sintered metal powder layer so consolidating the deposit before another layer is added. The item is then built up, layer-by-layer to create a net-shaped part. This revolutionary rapid prototyping process can now be used to create finalized spacecraft parts with a 40 % weight saving. Some improvements in the chemical purity of the powders used should increase yields to 100 % and, already, a 3D printer is in operation on the International Space station. This “first” 3D printing in space was performed in December 2014 by Butch Wilmore as part of a Zero gravity demonstration—engineers up-linked a custom-made digital design file of a ratchet wrench to the 3D printer and produced a tool measuring 11.4 cm in length. This process will enable fragile items to be “manufactured in space” without the need to incorporate “robustness” and extra weight for surviving the shocks, vibration and mechanical loads encountered during launch. The deposition of materials can be so-called, functionally graded, permitting one face of the deposit to have totally different properties when compared to the opposite

face. Similarly, custom compositions can be 3D printed so that undesirable compositions (possibly brittle intermetallic compounds, magnetic phases or corrodible compounds) in any binary or ternary phase diagram can be avoided by only depositing the useful compositions. The waste-, weight- and money-saving attributes of AM have already attracted manufacturers in all fields of advanced technology to incorporate AM into the production lines for their customized parts. These include heat-resistant bosses for turbine cases, large bearing housings, rocket engine injectors, landing gear support struts, and numerous spare parts.

Creative endeavors, like that noted in Fig. 2.3, may even enable additive layer manufacturing (ALM) to print a habitable structure on the Moon (Redahan 2014). Figure 2.3a illustrates how functional habitation modules could be brought from Earth; the surface of the thin-walled inflatable structures would then be coated by 3-D printing a powder made entirely of regolith, having a particle size of around 200 μm , onto the thin-wall until a sufficiently large wall thickness could be built up to protect human space-workers from radiation and micrometeoroids. Regolith is the name given to lunar dust and this local resource has already been encountered by humans and analyzed with respect to particle size and composition (see Fig. 2.3b, c). Quantitative optical and electron-probe studies by the UK Institute of Geological Sciences (Simpson 1970) have shown that lunar samples can contain ilmenite, pyroxene, chrome-titanium spinel, troilite, native iron, iron-nickel alloy, and even native copper (as shown in Fig. 8.1). This concept for constructing a human outpost on the Moon using lunar soil, and ways to monitor the buildings’ progress from Earth by means of an industrial CCD camera positioned on the printer, have been described by Ceccanti (2010) and Colla (2014).

Another rapid prototyping process that demonstrates great promise has been described by Maxwell et al. (2013). Known as Hyperbaric Pressure Laser Chemical Vapour Deposition (HP-LCVD), this rapid prototyping process incorporates a mixture of reactive gases into which laser beams penetrate for the growth of materials from atomic level to large structures by means of thermally- or photolytically-induced decomposition of the gaseous precursor. Exploitation of this HP-LCVD process, as prescribed by Dynetics and the NASA Marshall Space Centre (Maxwell et al. 2013), may enable 3D rapid prototyping in-space for the fabrication of components, replacement parts and even nuclear thermal propulsion systems—by the use of precursor gases and raw materials found, often in abundance, within our own Solar System.

Numerous advanced materials and manufacturing techniques will be individually described in Chap. 4.

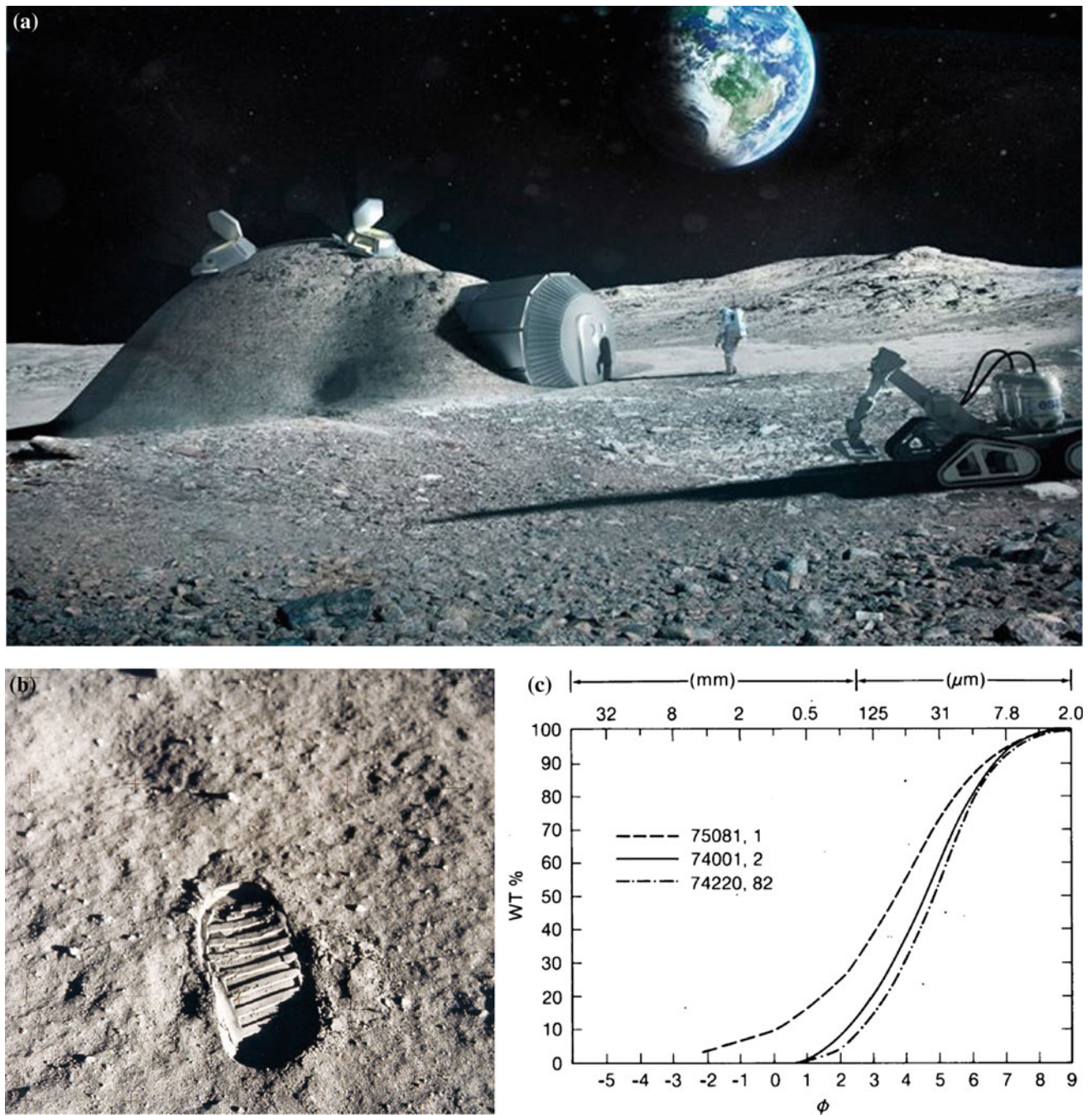


Fig. 2.3 **a** An artist's impression of an igloo, built on the Moon by means of a 3D printer attached to the arm of the robotic vehicle seen to the *right*. Printing powder material is Moon dust (regolith), processed into a cell-like structure of high strength—the idea is to initially inflate a thin folded dome brought from Earth and protect it with a cellular shell using the 3D printer—the pressurised enclosure so shields astronauts from solar radiation, micrometeorites and severe thermal

cycling. Concept and illustration courtesy of ESA and architects Foster + Partners. **b** Apollo 11 astronaut's footprint in lunar soil, made up of small, dust-like particles of regolith (*courtesy* NASA photo AS11-40-5877). **c** Grain size distribution of lunar soil from three different sites; about 50 % is greater than 100 μm from Heiken et al. (1974)

Table 2.1 Static corrosion potential of metals and alloys (de Rooij 1989a)

Material	EMF Potential
The metals having the greater negative EMF will tend to corrode and form oxides	EMF between a calomel electrode and a 3.5 % NaCl water solution (V)
Platinum	+0.17
Carbon	+0.15
Gold	+0.15
Rhenium	+0.08
Rhodium	+0.05
Tantalum	+0.04
Silver	−0.03
Ag10Cu braze alloy	−0.06
A286 (15Cr, 25Ni, Mo, Ti, V) passive	−0.07
AISI 316 (18Cr, 13Ni, 2Mo, rem Fe) passive	−0.07
AISI 321 (18Cr, 10Ni, 0.4Ti) passive	−0.08
AISI 347 (18Cr, 12Ni, +Nb, rem Fe) passive	−0.08
AISI 301 (17Cr, 7Ni) passive	−0.09
AISI 304 (19Cr, 10Ni, rem Fe) passive	−0.10
Hastelloy C (17Mo, 15Cr, 5W, 6Fe, rem Ni) passive	−0.10
Nichrome (80Ni, 20Cr) passive	−0.10
Monel 60 (65Ni, 0.2Fe, 3.5Mn, 2Ti, 27Cu)	−0.10
Inconel 92 (71Ni, 16Cr, 7Fe, 3Ti, 2Mn) passive	−0.11
17-7PH stainless st. (17Cr, 7Ni, 1.1Al) passive	−0.11
AISI 309 (23Cr, 13Ni) passive	−0.11
Titanium	−0.12
Monel 400 (32Cu, 2.5Fe, 2Mn, rem Ni)	−0.12
CDA 442 (71Cu, 1Sn, 38Zn)	−0.12
CD A 715 (70Cu, 30Ni)	−0.12
Molybdenum	−0.12
MP35N (Ni, 35Co, 2.0Cr, 10Mo) passive	−0.15
CDA 510 (96Cu, 4Sn, P) phosphor bronze	−0.16
AISI 420 (0.35C, 13Cr, rem Fe) passive	−0.17
AISI 434 (0.12C, 17Cr, 1Mo, rem Fe) passive	−0.17
Bismuth	−0.17
Waspaloy (59Ni, 19.5Cr, 13.5Co, 4Mo) passive	−0.17
Nickel passive	−0.18
Monel 67 (67.5Cu, 31Ni, 0.3Ti, 0.5Fe)	−0.18
Copper phosphorus (4.5P, rem Cu)	−0.18
Copper phosphorus (8.5P, rem Cu)	−0.19
Copper phosphorus (10.5P, rem Cu)	−0.20
Copper	−0.20
CDA 110 (electrolytic tough pitch)	−0.20
CDA 172 (2Be, rem Cu)	−0.20
Gold-germanium solder (12Ge, rem Au)	−0.20
Copper-Gold (25Au, rem Cu)	−0.20
AISI 440B (17Cr, 0.5Mo, rem Fe) passive	−0.23

(continued)

Table 2.1 (continued)

Material	EMF Potential
The metals having the greater negative EMF will tend to corrode and form oxides	EMF between a calomel electrode and a 3.5 % NaCl water solution (V)
Ti6Al4 V (6Al.4 V, rem Ti)	-0.24
Silicon	-0.24
Tungsten carbide (94WC, 6Co)	-0.25
CDA 240 (80Cu, 20Zn)	-0.25
CDA 220 (90Cu, 10Zn)	-0.25
CDA 752 (65Cu, 18Ni, 17Zn)	-0.25
CDA 180 (60Cu, 40Zn)	-0.26
CDA 464 (60Cu, 1Sn, 39Zn)	-0.26
CDA 270 (63Cu, 37Zn)	-0.26
CDA 298 (52Cu, 48Zn)	-0.27
Nichrome 80/20 (80Ni, 20Cr) active	-0.27
CDA 521 (7Sn, rem Cu)	-0.27
CuAl10Fe (10Al.3Fe, rem Cu)	-0.27
Armco 21-6-0 (22Cr, 12Ni, rem Fe)	-0.27
Inconel 92 (71Ni, 16Cr, 7Fe, 3Ti, 2Mn) active	-0.28
CuAl12 (12Al, rem Cu)	-0.29
Niobium (1Zr, rem Nb)	-0.30
Tungsten	-0.30
Nickel active	-0.30
Kovar, Nilo 'K' (29Ni, 17Co, rem Fe)	-0.30
Chromium active	-0.31
Cobalt	-0.32
Nitinol (45Ti, 55Ni)	-0.33
Invar (36Ni, rem Fe)	-0.38
Cerrotrac (42Sn, rem Bi)	-0.39
SnAg4C3.5 solder	-0.42
Sn95Ag4.9In0.1 solder	-0.43
SnAg4 solder	-0.46
SnAg5 solder	-0.46
Tin	-0.46
Sn10Sb solder	-0.48
Indalloy no. 10 (75Pb.25In) solder	-0.48
Indalloy no. 7 (50Pb.50In) solder	-0.49
Lead	-0.50
Sn63 (63Sn, 37Pb) solder	-0.51
Sn60 (60Sn, 40Pb) solder	-0.51
Sn62Ag2 (62Sn, 36Pb, 2Ag) solder	-0.51
Sn59Sb2 (59Sn, 39Pb, 2Sb) solder	-0.51
Sn60Sb5 (60Sn, 35Pb, 5Sb) solder	-0.51
Sn60Sb10 (60Sn, 30Pb, 10Sb) solder	-0.51
Sn60Pb39.5Cu0.12P0.9 solder	-0.51
PbSn5Ag1.5 solder	-0.51
Mild steel	-0.52

(continued)

Table 2.1 (continued)

Material	EMF Potential
The metals having the greater negative EMF will tend to corrode and form oxides	EMF between a calomel electrode and a 3.5 % NaCl water solution (V)
AISI 304 (19Cr, 10Ni, rem Fe) active	-0.52
AISI 420 (0.35C, 13Cr, rem Fe) active	-0.52
AA 2219-T3.T4 (6.3Cu, 0.3Mn, 0.18Zr, 0.1V, 0.06Ti, rem Al)	-0.56
AISI 440B (17Cr, 0.5Mo, rem Fe) active	-0.59
AA 2014-T4 (4.5Cu, 1Fe, 1Si, 0.15Ti, rem Al)	-0.61
AA 2017-T4 (4Cu,1Fe,1 Mg,0.1Cr,rem Al)	-0.61
AA 2024-T3 (4.5Cu, 1.5 Mg, 0.6Mn, rem Al)	-0.62
AA B295.0-T6 (2.5Si, 1.2Fe, 4.5Cu, rem Al) casting	-0.63
In75Pb25 solder	-0.64
Indalloy No. 1 (50In, 50Sn) solder	-0.65
AA 380.0-F (8.5Si, 2Fe, 3.5Cu, rem Al) casting	-0.66
AA 319.0-F (6Si, 1Fe, 3.5Cu, rem Al) casting	-0.66
AA 333-0-F (9Si.1Fe, 3.5Cu, rem Al) casting	-0.66
Indium	-0.67
AA 2014-T6 (4.5Cu, 1Fe, 1Si, 0.15Ti, rem Al)	-0.69
Cadmium	-0.70
AA 2024-T81 (4.5Cu, 1.5Mg, 0.6Mn, rem Al)	-0.71
AA 2219-T6,T8 (6.3Cu, 0.3Mn0.18Zr, 0.1V, 0.06Ti, rem Al)	-0.72
AA 6061-T4 (1 Mg, 0.6Si, 0.25Cu, 0.2Cr, rem Al)	-0.72
AA 4043 (12Si, 1Cu, 1Mg, rem Al)	-0.74
AA 6151 (1 Mg, 1Fe, 0.25Sn, 0.15Ti, rem Al)	-0.74
AA 7075-T6 (5.6Zn, 2.5Mg, 1.6Cu, 0.3Cu.03Cr, rem Al)	-0.74
AA 7178-T6 (6.8Zn, 32Mg, 2Cu, 0.2Ti, rem Al)	-0.74
AA 1160 (98.4Al)	-0.75
Aluminium	-0.75
AA 5356 (5Zn, 0.1Ti, 0.1Cr, rem Al)	-0.75
AA 5554 (5 Mg, 1Mn, 0.25Zn, 0.2Cr, rem Al)	-0.75
AA 1050 (99.5Al)	-0.75
Al-3Li	-0.75
AA 1100 (99.0Al)	-0.75
AA 3003 (1.2Mn, rem Al)	-0.75
AA 6151 (1Mg, 1Fe,0.8Mn, 0.25Zn, 0.15Ti, rem Al)	-0.75
AA 6053 (1.3Mg, 0.5Si, 0.35Cr, rem Al)	-0.75
AA 6061-T6 (1Mg, 0.6Si, 0.25Cu, 0.2Cr, rem Al)	-0.75
AA 6063 (0.7Mg, 0.4Si, rem Al)	-0.75
Alclad 2014 (4.5Cu, 1Fe, 1Si, 0.15Ti, rem Al)	-0.75
Alcald 2024 (4.5Cu, 1.5Mg, 0.1Cr, rem Al, Al-clad)	-0.75
AA 3004 (1.5Mn, rem Al)	-0.76
AA 1060 (99.6Al)	-0.76
AA 5050 (1.5Mg, rem Al)	-0.76
AA 7075-T73 (5.6Zn,2.5 Mg,1.6Cu,0.3Cr,rem Al)	-0.76
AA 5052 (2.5Mg, 0.25Cr, rem Al)	-0.77
AA 5086 (4Mg, 0.5Mn, rem Al)	-0.77

(continued)

Table 2.1 (continued)

Material	EMF Potential
The metals having the greater negative EMF will tend to corrode and form oxides	EMF between a calomel electrode and a 3.5 % NaCl water solution (V)
AA 5154 (3.Mg, 0.25Cr, rem Al)	−0.78
AA 5454 (2.8Mg, 1Mn, 0.2Ti, 0.1Cu, 0.2Cr, rem Al)	−0.78
AA 4047 (12Si, rem Al)	−0.78
Al-C	−0.78
AA 5056 (5.2Mg, 0.1Mn, 0.1Cr, rem Al)	−0.79
AA 7079–T6 (4.3Zn, 3.3Mg, 0.6Cu, 0.2Mn, 0.2Cr, rem Al)	−0.79
AA 5456 (5Mg, 0.7Mn, 0.15Cu, 0.15Cr, rem Al)	−0.79
AA 5083 (4.5Mg, 0.7Mn, rem Al)	−0.79
AA 7072 (1Zn, 0.5Si, 0.3Cr, rem Al)	−0.87
Beryllium	−0.97
Zinc	−1.03
Manganese	−1.21
Erbium	−1.34
Electron (4Zn, 0.7Zr, rem Mg)	−1.55
ZW3 (3Zn, 0.5Zr, rem Mg)	−1.57
AZ61 (6Al, 1Zn, 0.3Mn, rem Mg)	−1.57
AZ31B (3Al, 1Zn, rem Mg)	−1.60
Magnesium	−1.60
HK31A (0.7Zr, 3Th, rem Mg)	−1.61

Notes to Table 2.1

Compatible material couples are considered to have a maximum potential difference of 0.25 V for non-cleanroom environments

0.50 V for cleanroom or hermetically sealed environments

This galvanic series chart is useful for a first approximation in selecting materials for corrosion control, but may be too simplistic for further dependence. It provides no information concerning corrosion rates or what will happen when three or more metals are electrically coupled. Service conditions such as ionic concentration, aeration, metal purity, etc. can change relative positions. Reversals, especially with metals that are very close in the series, such as steel and aluminium, can cause serious service problems, and specialized polarization studies are then recommended. The majority of alloys present in this Table can be referred to in Appendix 6 which lists specification number, composition limits and equivalent British, French, German and US standards

2.2.3 Some Basic Considerations Regarding Corrosion Prevention

It is necessary to ensure that any newly selected material will retain its functional properties during all stages of the spacecraft's designed life, up to the end of the mission. During manufacturing, the material must not degrade because of contamination from processing steps such as the release agents used for items moulded from CFRP, or by cutting oils used in the machining of alloys. Galvanic and general surface corrosion must be avoided during environmental testing and ground storage by the correct selection of surface finishes such as anodic films, chemical conversion films, and paints. When electrical grounding is required, only contacts having a compatible coupling of less than 0.5 V should be chosen. The static corrosion potential for a large number of metals and alloys has been established (de

Rooij 1989a) and is presented in Table 2.1. However, de Rooij has simplified this Table into Groupings of metallic alloys and the modified tabulation now appears as shown in Table 2.2. The material may need a high resistance to Stress Corrosion Cracking (SCC) before launch, and in such cases can be selected from those alloys listed in Table 2.3.

The primary and secondary structures will be made from light alloys based on aluminium and magnesium, together with titanium and to a very limited extent beryllium. Nickel alloys are often selected for their high-temperature performance and oxidation resistance; they are often known by trade names, rather than by their specification code numbers. Commercially pure nickel, easy to form into complex shapes, is used in the construction of spacecraft electronics where its electrical and magnetic properties are crucial. Mechanical designers often select Inconel alloys 600 and 625 because they appear in Table 2.3, but it has recently

Table 2.2 Suggested compatible couples for bimetallic contacts (after de Rooij, based on Table 2.1)

Pure metals and alloys in alphabetical order (including carbon)	Aluminium-copper alloys	Al (pure), Al-zinc alloys	Cadmium	Cast iron (austenitic)	Chromium	Copper, brasses	Cupro-nickel, Al-bronzes, Si-bronzes	Gold, platinum, carbon, rhodium	Gun-metal (CuZn10 alloy), P-bronzes, Sn-bronzes	Magnesium	Nickel, monel, inconel, Nickel/molybdenum-alloys	Silver	Sn-Pb alloys (all, tin, lead	Stainless steel 18/8 (300 series)	Stainless steel 13Cr (400 series)	Steel (carbon, low alloy), Cast iron	Titanium and Ti-alloys	Zinc, beryllium
Aluminium-copper alloys		1	1	3	3	3	3	3	3	2	2	3	1	2	2	3	2	2
Al (pure)			1	3	3	3	3	3	3	2	3	3	2	3	3	3	3	2
Al-Zinc alloys																		
Cadmium				2	2	2	2	2	2	1	2	2	0	1	1	2	2	2
Cast iron (austeni)					1	1	1	2	1	3	1	2	1	1	1	2	1	3
Chromium						1	0	0	1	3	1	0	2	0	0	2	0	3
Copper, brasses							0	2	0	3	1	1	2	1	1	3	0	3
Cupro-nickel																		
Al-bronzes								2	0	3	1	1	2	2	1	3	0	3
Si-bronzes																		
Gold																		
platinum,																		
carbon																		
rhodium									2	3	2	0	3	0	1	3	0	3
Gun-metal(CuZn10 alloy)																		
P-bronzes										3	1	1	1	0	0	3	0	3
Sn-bronzes																		
Magnesium											3	3	2	3	3	3	3	3
Nickel																		
monel																		
inconel												2	2	1	0	2	1	3
nickel/molybdenum-alloys																		
Silver													3	0	0	3	0	3
Sn-Pb alloys (all)														1	1	1	3	1
tin, lead																		
Stainless steel 18/8 (300 series)															1	3	0	3
Stainless steel 13Cr (400 series)																3	0	3
Steel (carbon, low alloy)																	0	3
cast iron																		
Titanium and Ti-alloys																		3
Zinc																		
beryllium																		

Key

0—Can be used without restriction

1—Can be used in a non-controlled environment (e.g. assembly area and general non-clean room environment)

2—Can be used in a clean room environment

3—Need specific measures to avoid corrosion when these combinations are selected

Table 2.3 Alloys with high resistance to stress-corrosion cracking

Steel alloys			
Alloy		Condition	
Carbon steel (1000 series)		Below 180 ksi UTS	
Low alloy steel (4130, 4340, D6AC, etc.)		Below 180 ksi UTS	
Music wire (ASTM 228)		Cold drawn	
1095 spring steel		Tempered	
HY 80 steel		Tempered	
HY 130 steel		Tempered	
HY 140 steel		Tempered	
200 series stainless steel (unsensitized)		All	
300 series stainless steel (unsensitized) ^a		All	
400 series ferritic stainless steel (404, 430, 444, etc.)		All	
Nitronic 32		Annealed	
Nitronic 33 ^b		Annealed	
Nitronic 40 (formerly 21-6-9) ^b		Annealed	
A-286 stainless steel		All	
AM-350 stainless steel		SCT 1000 and above	
AM-350 stainless steel		SCT 1000 and above	
AM-362 (Almar 362) stainless steel		3 h. at 1000 °F	
Carpenter 20Cb-3 stainless steel		All	
Carpenter 20Cb-3 stainless steel		All	
Custom 450 stainless steel		H1000 and above	
Custom 455 stainless steel		H1000 and above	
15-5PH stainless steel		H1000 and above	
PH15-7Mo stainless steel		CH900	
17-7PH stainless steel		CH900	
Aluminium alloys			
Wrought		Cast	
Alloy ^c	Temper ^d	Alloy ^e	Temper
1000 series	All	319.0, A319.0	As cast
2011	T8	333.0, A333.0	As cast
2024 rod, bar	T8	355.0, C355.0	T6
2219	T6, T8	356.0, A356.0	All
2418	T8		
2618	T6	357.0	All
3000 series	All	B358.0 (Tens-50)	All
5000 series	All ^{f, g}	359.0	All
6000 series	All	380.0, A380.0	As cast
7049	T73	514.0 (214)	As cast ^g
7149	T73	518.0 (218)	As cast ^g
7050	T73	535.0 (Almag.35)	As cast ^g

(continued)

Table 2.3 (continued)

Aluminium alloys			
7050	T73	A712.0, C712.0	As cast
7475	T73		
Copper alloys			
CDA No. ^h		Condition (% cold rolled) ⁱ	
110		37	
170		AT, HT. ^j	
172		AT, HT. ^j	
194		37	
195		90	
230		40	
280		0	
422		37	
443		10	
510		37	
521		37	
524		0	
606		0	
619		40 (9 % B phase)	
619		40 (95 % B phase)	
655		0	
688		40	
704		0	
706		50	
710		0	
715		0	
725		50 Annealed	
Nickel alloys			
Alloy		Conditions	
Glass Seal 52 CR (51Ni-49Fe)		All	
Invar 36 (36Ni-64Fe)		All	
Hastelloy B		Solution heat treated	
Hastelloy C		All	
Hastelloy X		All	
Incoloy 800		All	
Incoloy 901		All	
Incoloy 903		All	
Inconel 600		Annealed	
Inconel 625		Annealed	
Inconel 718		All	
Inconel X-750		All	
Monel K-500		All	
Ni-Span-C 902		All	
Rene 41		All	

(continued)

Table 2.3 (continued)

Nickel alloys	
Unitemp 212	All
Waspaloy	All
Miscellaneous alloys	
Alloy	Conditions
Beryllium S-200C	Annealed
HS25 (L605)	All
HS 188	All
MP35 N	Cold worked and aged
MP159	Cold worked and aged
Titanium 3Al-2.5 V	All
Titanium 5Al-2.5SN	All
Titanium 6Al-4 V	All
Titanium 10Fe-2 V-3Al	All
Titanium 13V-11Cr-3Al	All
Titanium IMI 550	Al
Magnesium MIA	All
Magnesium LA141	Stabilized
Magnesium LAZ933	All

^aIncluding weldments of 304L, 316L, 321 and 347

^bIncluding weldments

^cIncluding weldments of the weldable alloys

^dMechanically stress relieved (TX5X or TX5XX) where specified

^eThe former designation is shown in parentheses where significantly different. See Appendix 5 for temper designations

^fHigh magnesium alloys 5456, 5083, and 5086 should be used in controlled tempers (H111, H112, H116, H117, H323, H343) for resistance to SCC and exfoliation

^gAlloys with magnesium content greater than 3.0 percent are not recommended for high-temperature application, 66°C (150°F) and above

^hCopper Development Association alloy number

ⁱMaximum percent cold rolled for which SCC data are available

^jAT—annealed and precipitation hardened

HT—work hardened and precipitation hardened

Notes to Table 2.3

Data are compiled from NASA MSFC Spec 522B and ECSS-Q-ST-70-36. Recent issues of these documents should be consulted for classification of alloys with both a moderate and a low resistance to stress corrosion cracking. Appendix 5 describes the aluminium alloy temper designations. A search through Appendix 6 will indicate similar European alloys

been acknowledged that these alloys soften, and can suffer from SCC in pure water, at temperatures above 300 °C (steam generators for nuclear plants). It may be wiser to use a development of the 625 alloy when high temperatures may be expected, for instance in propulsion systems. This development involved the additions of molybdenum and niobium to 625 to impart solid solution hardening and the formation of Ni₃Nb, a very effective hardening precipitate. This is known as the super alloy Inconel 718 and has become the most widely used high temperature nickel alloy.

All the classical assembly methods are employed: welding, brazing, soldering, riveting, bolting, and adhesive bonding. It is important to ensure the joining processes themselves have not degraded the materials' surface or stress corrosion resistance. (Heating can modify an alloy's microstructure, weld metal and heat affected zones will be different to the parent metal, braze metal may be noble to the remaining surfaces which can preferentially corrode, mechanical joints can have re-entrant faces that retain water and cause pitting, even cured resins may release acids that damage the surrounding surfaces). Generally, aircraft industry manufacturing standards are followed, and much attention is given to process control and there is a need to evaluate all process used to join together structural and electrical parts.

2.2.4 Space Project's Phases and Management Events

It is important to note that before a satellite becomes fully operational in orbit its subsystems, mechanisms, and electronics will have been subjected to the following main environmental conditions:

(A) Ground activities:

Operation for test and checkout
Handling
Transportation
Storage
Exposure to the elements

(B) Subjection to launch and ascent:

Acceleration and shock
Vibration and acoustic noise and possibly contact with reactive fuels, oxidizers, and temperature extremes
Pyrotechnic shock

(C) Transfer to operational orbit position:

Thermal cycling due to exposure to the Sun and eclipse
Ultrahigh vacuum
Radiation—electromagnetic and penetrating particles
Zero gravity

The new millennium saw a great increase in the size and complexity of spacecraft. This has necessitated ground testing facilities to become modernized, physically larger, and more sophisticated for the exposure of space hardware to the environments listed in A to C above. The Test Facility within space agencies are comprised of high capital investments such as Large Space Simulators that reproduce the vacuum, certain radiations and the cryogenic-to-elevated temperatures encountered by space hardware. Mechanical and acoustic tests simulate the launch environment, the magnetic

characteristics of spacecraft are evaluated and all tests are performed under various classes of cleanroom conditions.

As mentioned previously, a development plan for a new spacecraft design will involve a ‘model philosophy’ where models of the craft will be dynamically tested—without testing the risk of failures is too great. In the early days it was not uncommon for space authorities to build four models for testing prior to actually building a flight spacecraft. The model philosophy will be accounted for in the next paragraph, but it is emphasised that as the space industry has matured, the design margins have become established (for structures and electronic systems) so that there is now more focus on analysis and less on actual testing. It is now the norm to build only one prototype for testing—often this ‘build and test’ is completed only six months before work commences on manufacturing the flight spacecraft.

It is interesting to remember the aims of the ‘model philosophy’ for the early (70’s and 80’s) European telecommunication satellite projects. The *structural model* was subjected to a programme of tests which exceeded the expected launch environment conditions (each type of launch vehicle has its own characteristic levels of vibration and acoustic noise). Typical test configurations are shown in Fig. 2.1a–c. The enormous amount of energy released during launch can be witnessed from Fig. 2.2. Weakness in designs may be exposed by this model, such as failures resulting from fatigue of welds, struts, electronic box hold-down points, and the like. The *thermal model* was subjected to solar simulation and thermal balance testing to confirm and update previously determined mathematical models. During these tests, deficient designs may promote several material failures related to thermal fatigue, overheating, and embrittlement of incompatible joining techniques and metal alloys. By simply modifying the paint finish of the spacecraft surface, or by the attachment of reflective mirrors, it was found possible to adjust and reduce the local temperature environment of each subsystem or equipment and reduce the chance of thermally induced failures. Workmanship problems abounded, with non-conformances relating to open circuits in cable harnesses due to wires separating from crimp barrels and cold soldered joints on circuit boards (such events became less frequent once operator and inspector training schemes were introduced—see Sect. 6.14). The *engineering model* ensured that integration and performance could be achieved. A review of the old project and laboratory failure investigation reports was made by the author (at the time of filing and archiving as a result of which they were lost forever!). This revealed that several material problems only came to light during integration, particularly at the mechanical interfaces between equipments and the structure (e.g. failure of springs and bolting devices due to incorrect plating processes which cause delayed failure by hydrogen embrittlement; the over-torqueing and fracture of lock-nuts

and other operator handling errors, etc.). It was seen that the reliability of electrical interfaces between equipments, and the mutual compatibility between the constituent subsystems, was seriously jeopardized by fundamental oversights (e.g. high electrical resistance between gold-plated and aluminium-finished interfaces due to galvanic corrosion; migration of silver to produce short circuits; the use of austenitic steels having work-hardened and therefore slightly magnetic surfaces in locations required to be magnetically clean; etc.). Remedial actions were taken by suppliers and assemblers as a result of failure review boards (FRBs). Lessons learnt documents (nowadays called internal problem notification documents—IPNs) were written and circulated. Finally, a fully assembled *qualification model* was built and subjected to a comprehensive series of environmental ground tests. These usually included: sine vibration, spin, acoustic noise vibration, centrifuge acceleration, and solar simulation. Each of these major test phases was preceded by an integrated systems test in order to verify that the functional behaviour of the satellite was correct. It was not uncommon that the qualification model would be recognized as a “flight spare” in case of launcher failure.

Flight model test programmes were, and continue to be, more limited than those used on the qualification model (most customers now refer to this as the protoflight model).

It may be assumed that some subsystem parts that will operate for relatively short periods after launch can accumulate several hundred hours of test operation before the actual time of launching. Materials selected for use under the vacuum conditions of space may therefore have to operate for periods under normal atmospheric conditions. This may create special problems. One is immediately reminded that very thin (tens of Ångströms¹) films of lead, or molybdenum disulphide, for the lubrication mechanisms, can rapidly oxidize under terrestrial conditions and become the cause of malfunction. This goes to illustrate the need to know the effects that ground testing may have on delicate surfaces.

A final concern of the writer relates to the participation of materials experts on spacecraft project review boards. It is paramount that an experienced materials engineer is incorporated into each of the four major reviews during the design and construction of individual spacecraft. Whenever ECSS Q-ST-70 is included as a contractual document this become a requirement—as a minimum, the materials engineer will manage the steps taken for the project-approval of declared lists for every flight material, mechanical part and their related processes (i.e. DML, DMPL and DPL). Tasks should also include cleanliness and contamination control, the testing and validation of new materials, assistance in the

¹1 Å equals 10^{-10} m.

qualification of mechanical parts and the verification of new or critical processes.

Spacecraft, such as CubeSats and university flight experiments may follow less rigorous requirements and a reduced M&P programme is suggested in Appendix 8.

Reviews are usually contractual milestones and essentially question: will the design, hardware, software, and operational approach satisfy the mission objectives? The review names and their main objectives are as follows:

PDR (preliminary design review): after evaluation of thermal and/or engineering models, to approve and release the preliminary design, including materials and processes.

CDR (critical design review): this establishes the final design and agrees that flight hardware manufacturing can commence (all declared materials being approved and production process, when required, are verified as being suitable).

QR (qualification review): assess that all qualification activities on subsystems are complete—for certain projects a qualification model is built.

LRR (launch and operations readiness review): this checks that all lower-level acceptance reviews have been successfully completed, the flight model spacecraft accepted, and it is then authorized to be launched.

(b) Sublimation and evaporation

The minimum altitude for an Earth-orbiting satellite is 200 km (125 miles), and, once this altitude has been reached, appreciable changes can be produced in common engineering materials, whether they be metals, plastics, or ceramics. The vacuum in space is very high, the pressure falling from 10^{-6} mm Hg at 200 km to less than 10^{-12} mm Hg beyond 6500 km. Some polymers will decompose and some metals will tend to sublime under vacuum. The rate at which the molecules or atoms leave a surface in vacuum will rise rapidly with an increase in temperature according to the equation:

$$G = 5.04 \times 10^3 P(M/T)^{1/2}$$

where

G grams of material evaporated or sublimated per square centimetre per day

P Vapour pressure of the evaporating species in torr²

M Molecular weight of the material

T Absolute temperature, K

Temperature has an enormous effect on the amount of metallic material that is sublimated. As examples, cadmium and zinc have sublimation rates that increase by a factor of ten for roughly every 30 °C rise in temperature:

Cadmium has a vapour pressure of 10^{-8} at 70 °C (approximately)

10^{-7} at 90 °C

10^{-6} at 120 °C

10^{-5} at 150 °C and

10^{-4} at 180 °C

The relationship between the vapour pressure of a metal (P) and temperature (T) is given by the following equation:

$$P = P_{\infty} e^{-E/RT}$$

where P_{∞} = a constant (i.e. vapour pressure at $T = \infty$), E = heat of evaporation (e.g. joule · mole⁻¹), and R = gas constant (8.3 J mol⁻¹ K⁻¹).

The temperatures for given metallic **sublimation rates** are listed in Table 2.5. The thermal environment in space is completely different from thermal conditions on Earth. Without an atmosphere, the only means of exchanging thermal energy is by thermal radiation and conduction. Certain parts of satellites have been calculated to follow

2.3 The Effect of a Space Environment

(a) General

The purpose of this section is to provide the reader with an overview of the salient points concerning the effect of a space environment on spacecraft parts and materials. Far greater discussion with examples will be made of these effects throughout the remainder of this book.

Each spacecraft material will be required to suffer no vibrational fatigue damage during the launch. In orbit, it will need to survive the space environment (see Table 2.4) and, in particular, to possess low-outgassing-under-vacuum properties, whether it be a lubricating grease or a structural plastic. Radiation and thermal cycling must not degrade thermal-control surfaces or joints in materials possessing different coefficient of expansion. The presence of atomic oxygen in low Earth orbits, a relative newcomer in environmental effects, has been seen to lead to the erosion/corrosion/oxidation of many material surfaces, and more coatings with good atomic oxygen durability need to be developed. These aspects will be detailed in Chap. 8.

²The term 'torr' is generally used instead of 'mm Hg' by international agreement of several vacuum societies. 'Torr' honours the name of Torricelli, who discovered atmospheric pressure in 1643.

Table 2.4 Characteristics of the space environment—order of magnitude only (Dauphin 1984)

Altitude (km)	Pressure (mm Hg or torr)	Kinetic temperature (K)	Gaseous density (particle cm ⁻³)	Composition	Ultraviolet radiation	Particle radiation (particles cm ⁻² s ⁻¹)
Sea level	760	±300	2.5×10^{19}	78 % N ₂ , 21 % O ₂ , 1 % A	Section of solar spectrum 0.3	–
30	10	–	4×10^{17}	N ₂ , O ₂ , A	Absorption zone	–
200	10^{-6}	±1200	10^{10}	N ₂ , O, O ₂ , O ⁺	Full solar spectrum	–
800	10^{-9}	±1300	10^6	O, He, O ⁺ , H	Full solar spectrum	–
6500	10^{-13}	–	10^3	H ⁺ , H, He ⁺	Full solar spectrum	10 ⁴ protons 35 MeV 10 ⁴ electrons 40 keV
22,000	10^{-13}	–	10^1 – 10^2	85 % H ⁺ , 15 % He ²⁺	Full solar spectrum	10 ⁸ protons 5 MeV 10 ⁸ electrons 40 keV 10 ⁴ electrons 1.6 MeV

thermal excursions from approximately -160 to $+180$ °C. The actual temperature attained will differ from one spacecraft to another, the major temperature effect arising from the spacecraft's spin rate. Surfaces of non-spinning satellites exposed to direct solar radiation may be unable to dissipate thermal energy efficiently, and will reach higher temperatures than spinning satellites. Temperature variations will also depend upon the amount of albedo radiation and the amount of thermal radiation to space from the spacecraft. Both active and passive thermal control systems are employed on satellites in order to restrict the oscillating temperature extremes. The active systems have made use of thermostatically controlled heaters. Passive systems involve the surface absorptance/emittance, a/ϵ , properties of material finishes. Solar reflectors have low a/ϵ ratios, being generally white paints or clear anodized aluminium. Black paints and inorganic black anodized aluminium have a/ϵ values of approximately 1. Solar absorbers have an a/ϵ value greater than 1, and these are generally polished metals since the emittance values of uncoated metals are very low (<0.1). Examples are described in Sect. 5.5.

The majority of metals do not sublime at normal spacecraft temperatures. However, as can be seen in Table 2.5, cadmium and zinc must be excluded from use as they will readily sublime and could condense in the form of thin conductive deposits on electrical insulators, or opaque deposits on optical components which may be situated within the satellite or on its external surfaces. All cadmium, zinc, or tin-plated surfaces, such as the protective finishes on equipment or components including commercial connectors, must be avoided, because, as will be described in Chap. 7, they are known to grow single-crystal whiskers exceeding 2 cm length in vacuum. Extreme care must be taken to ensure that these metals are not used in the corrosion

proofing of any of the spacecraft's components. Magnesium parts could pose sublimation problems after long exposure to vacuum at temperatures greater than 125 °C, and experiments have shown (Frankel 1969) that magnesium sheets held at 230 °C and 1×10^{-7} mm Hg for only 168 h (one week) became severely pitted and dramatically decreased in static strength properties. Because of their relatively high strength-to-weight ratios, magnesium alloys are often employed as structural parts, but it is essential that these parts are finished with an adequate plating or chemical conversion coating which will prevent both the corrosion of the part before launch and the subsequent sublimation problem in orbit. Tin–lead alloys, such as those employed for soldering electrical components, have not been seen to sublime under spacecraft environments as they are restricted for use in areas which are thermally controlled to a maximum of about 80 °C. Solder alloys are used for joining silver-plated molybdenum interconnector strips between solar cells on the solar arrays of spinning satellites. As such satellites rotate, the maximum temperature of the arrays does not degrade the soldered joints. The stationary communication satellites will not be able to dissipate the absorbed thermal radiation on the solar arrays efficiently, so that welded interconnectors are necessary.

The events of sublimation and evaporation cause the release of metal atoms which travel and are capable of recondensing on cooler surfaces. They are readily ionized and may be contributors to corona and arcing phenomena. These metallic ions may also cause the complete failure of a satellite mission by recondensing between slip rings, causing electrical short circuits, or recondensing on optical surfaces causing the loss of a specific wavelength transmission. When such ions recondense on the spacecraft's highly reflective thermal control surfaces the thermal balance can be so

Table 2.5 Sublimation of metals and semiconductors in high vacuum

Sublimation rate	1000 Å ^a /year	10 ⁻³ cm/year (0.0004 in/year)	10 ⁻¹ cm/year (0.04 in/year)
Temperature	°C	°C	°C
Cadmium	40	80	120
Selenium	50	80	120
Zinc	70	132	180
Magnesium	110	170	240
Tellurium	130	180	220
Lithium	150	210	280
Antimony	210	270	300
Bismuth	240	320	400
Lead	270	330	430
Indium	400	500	610
Manganese	450	540	650
Silver	480	590	700
Tin	550	660	800
Aluminium	550	680	810
Beryllium	620	700	840
Copper	630	760	900
Gold	660	800	950
Germanium	660	800	950
Chromium	750	870	1000
Iron	770	900	1050
Silicon	790	920	1080
Nickel	800	940	1090
Palladium	810	940	1100
Cobalt	820	960	1100
Titanium	920	1070	1250
Vanadium	1020	1180	1350
Rhodium	1140	1330	1540
Platinum	1160	1340	1560
Boron	1230	1420	1640
Zirconium	1280	1500	1740
Iridium	1300	1500	1740
Molybdenum	1380	1630	1900
Carbon	1530	1680	1880
Tantalum	1780	2050	2300
Rhenium	1820	2050	2300
Tungsten	1880	2150	2500

^a1Å = 10⁻¹⁰ m

Based on data by Jaffe and Rittenhouse, California Institute of Technology

degraded that severe overheating will promote malfunctions. Cesium is an uncommon metal with a melting point of 28 °C and a boiling point of 671 °C but it has been proposed as a propellant for field effect electronic propulsion (FEEP) when very low thrust applications are required. Thrusters have

been developed using this metal, but CNES evaluations have determined that cesium can easily contaminate spacecraft surfaces due to its low vapor pressure and re-evaporate from surfaces warmer than -30 °C to cause further contamination and react chemically with polymers or some oxides to

change their optical properties (Tondou 2011). The BepiColumbo mission dedicated to the study of Mercury is a challenging ESA project where temperatures may reach 300 °C at all external surfaces and metallic sublimation is of major concern (as is the outgassing of organic materials). A reference to Table 2.3 will immediately show that materials containing zinc, cadmium (always prohibited in space applications) and lead are unsuitable candidates. Sublimation and cold welding of solar array drive mechanisms will require strict controls for the bearings, slip-rings and cables (Fink et al. 2009a, b).

For additional examples of the effect of sublimation on spacecraft hardware, the reader may refer to Sect. 5.6.

(c) *Radiation and particle damage*

Organic materials, such as those used for electrical insulation, may be damaged by ionization due to protons and electrons from radiation belts, solar emissions, and cosmic rays. The Van Allen radiation belt is especially damaging to organic materials and even inorganic materials which make up optical lenses, ceramic insulators, and sensitive electronic components. The metallic materials of most Earth-orbiting spacecraft, as well as deep-space probes, are unaffected by small particle radiations, and are only slightly degraded by erosion from a cloud of meteoric dust which surrounds the Earth and other planets. Larger particle damage was, however, a major problem for the Halley's Comet flyby mission—called Giotto—which encountered that comet in 1986. Special armour plating was developed to surround that spacecraft, which was impacted by rock debris travelling at hypervelocities of 10–70 km/s. These aspects are reviewed in Chap. 8.

(d) *Friction and wear*

One of the major material problem areas for advanced spacecraft is that of friction and wear of surfaces which must rub or slide over each other under conditions of temperature cycling and high vacuum. This may be encountered in the operation of hinges, gears, bearings, and electrical contacts used in a vast number of spacecraft mechanisms. During sliding under normal terrestrial conditions most contacting metallic surfaces are protected by a surface film of oxide, oil, grease, or other contaminant which will act as a 'shear layer' and prevent binding. Under vacuum conditions such contaminants outgas, and oxides, once disrupted or removed, are unable to reform. Also, the minute junction spots which carry the full load between contacting metallic surfaces will usually have vastly increased friction coefficients, and probably high rates of wear, so that many metallic couples will tend to cold-weld. It is usually

impracticable to enclose such moving parts within hermetically sealed containers, so special lubricants must be found which do not decompose or sublime under vacuum. Films of low shear strength, such as molybdenum disulphide or vacuum deposited soft metals (e.g. gold, lead, or silver), are most efficient, particularly when designed to be situated between hard substrates which will support the load and keep the contact area small.

The possibility of contacting metallic surfaces becoming cold welded to each other during, for instance, the operation of spacecraft mechanisms or loading of threaded fasteners under vacuum conditions depends on a number of factors; there will be a *greater chance* of cold welding if

- (a) the relative phase diagram indicates that the contacting metals or alloys form a solid solution with each other,
- (b) the metals are soft and have the same crystal structure,
- (c) contact surfaces are clean, or possess easily damaged/removable oxide films. Surface oxides are normally more brittle than metals and are therefore more likely to crack and expose underlying metal if it is too soft to provide a firm support under load, and
- (d) contact pressures are higher. The first step in order to minimize the possibility of cold welding is to select those metal combinations known to resist adhesive wear, as for instance those shown in Fig. 2.4a. The next step is to consider the surface finish.

Clean metallic surfaces react with the surrounding atmosphere to form oxides, nitrides, or other compounds that are held together by either strong chemical bonds, or weak van der Waals forces. These surface films reduce the possibility of metal–metal adhesion that would otherwise occur on intimate contact; they can be considered as naturally formed lubricating films. Under the space environment such films are unlikely to be self-healing if they become displaced. For this reason protective films of PTFE (Teflon), graphite, and molybdenum disulphide are frequently selected to prevent wear and cold-welding.

Suitable non-lubricated pairs of engineering alloys for sliding wear situations can be selected from engineering alloys having very different hardnesses—traditional reference books may be consulted (Brandes 1983; Lansdown and Price 1986), or for very precise data, the recent work of Merstallinger et al. (2009) can be checked for evidence of fretting wear and cold welding (it is intended that this reference work is maintained on the internet and updated as new pairs of engineering material pairs become tested).

In general, steels can be coupled with either copper alloys or steels of a different alloy type and hardness. Copper alloys can be coupled with chromium plating, high-chrome steels, and tungsten steels. Austenitic stainless steels have a

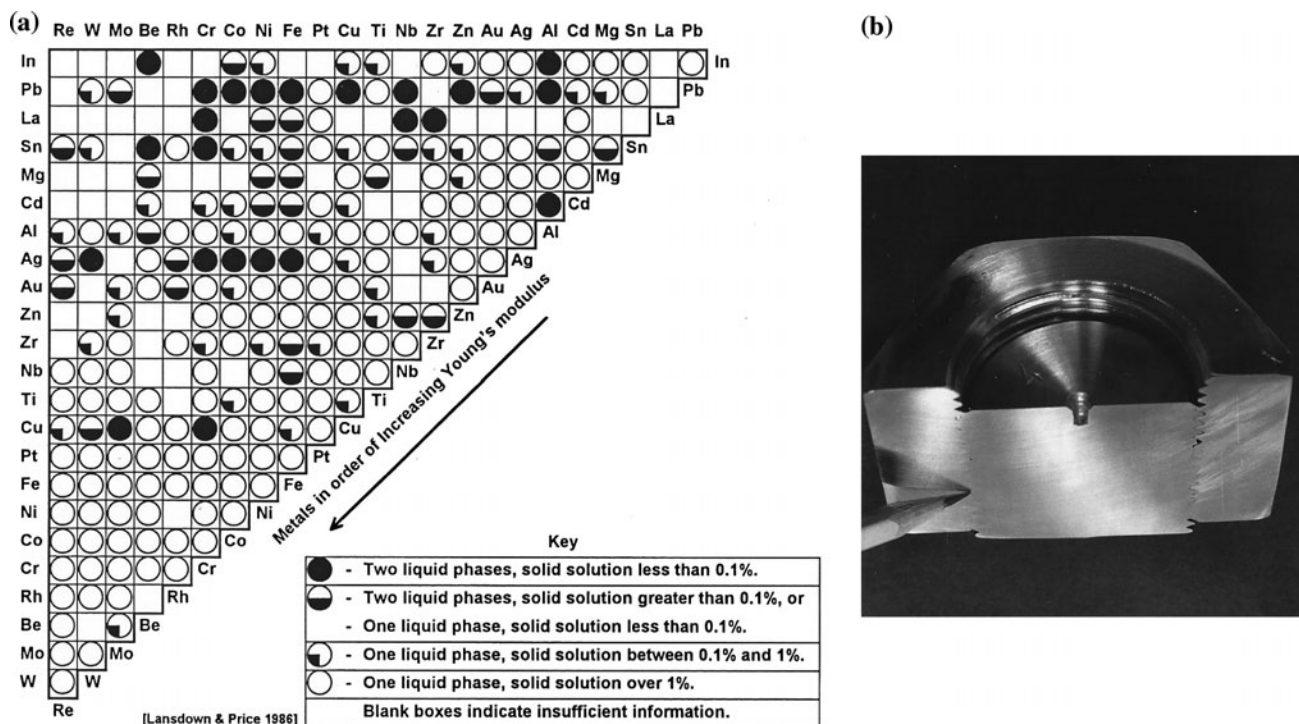


Fig. 2.4 **a** Depicts the theoretical possibility of clean metal surface pairs becoming cold-welded upon contact. Choice of a metal to resist adhesive wear with another specified metal. The “blacker” the circle, the better will be resistance to adhesive wear and cold welding under vacuum (Lansdown and Price 1986). Same-to-same metal contacts will result in solid solution, sticking and cold welding. **b** Demonstration of a case where “same metal” contacts have become cold welded (a form of solid state diffusion). By applying lead or silver coatings (e.g. as solid

lubricants) such sticking will be avoided. The very thin oxide film on austenitic stainless steel is easily ruptured under the sliding conditions of torquing-up nuts and bolts. High vacuum operation has contributed to the complete seizure by cold-welding of this 316 alloy vacuum chamber support fixture. The 45 mm diameter bolt was initially cut to release the threaded portion which was later cross-sectioned. The pointer shows the main region of cold-welded asperities

great tendency to cold-weld to each other (see Fig. 2.4) as they are both soft and unable to form thick protective chromium oxides. Alternatively, with very hard substrates such as chromium plating, surface deformation is so small that the surface chromium oxide film is never disrupted (see Fig. 2.5). Materials suitable for spacecraft bearing applications are titanium-carbide coated balls located in raceways fabricated from 440C or SAE 52100. A particularly good anti-wear surface, as for instance in gears, bushes, and pivots, is plasma-nitrided steel (Rowntree and Todd 1988). Thermal spraying is also a novel process for the coating of spacecraft subsystems enhancing wear resistance and as a thermal barrier—here thermal spraying can deposit both low and high melting point materials such as polymers and ceramics and metallic layers such as aluminium onto CFRP substrates such as antennae face-skins (Sturgeon and Dunn 2006; Saber-Samandari and Berndt 2010). Case histories related to wear are detailed in Sects. 5.2.7, 5.11, and 5.12. A large number of rules and design recommendations for the avoidance of wear and cold welding (for instance at mechanism end stops, hold-down and release springs, sliding contacts, and ball bearings) have been listed in the form of a

standard (Labruyère and Urmston 1995; Doyle and Hubbard 2010; ECSS-E-ST-32-08 2013).

It should be noted that all dry lubricants wear, and will possess a finite life. However, improved wear characteristics can be achieved by carefully selecting the process of applying the dry lubricant. Ion-plated lead and sputtered molybdenum disulphide are now well proven, having low coefficients of friction and a long life. Burnished or spray-bonded molybdenum disulphide has inferior friction properties. It is important to store the dry lubricated spacecraft mechanisms in a dry inert gas in order to prevent moisture pick-up, and as neither lead nor molybdenum disulphide perform well in air the number of operations in normal atmosphere should be restricted (Rowntree and Todd 1988).

(e) Cryogenic temperatures

All spacecraft structural metals will undergo changes in properties when cooled from normal ambient temperatures to temperatures in the ‘subzero’ range encountered during solar eclipse periods or when voyaging on deep-space missions. This will be an important factor when liquid helium



Fig. 2.5 Example of 300 mm long Spacelab pallet trunnion—machined from Inconel 718 and hard chromium plated. The insert shows plating to be 10 μm thick and well bonded to the etched substrate

cryostats form a major part of a payload, as for instance has been designed for the Infrared Space Observatory, where sophisticated instruments are located in a 60 cm telescope cooled to 2 K. The greater changes involve the embrittlement of metal alloys, particularly carbon steels. Space vehicles must be fabricated from materials with high strength-to-weight ratios. They must also be required to retain high levels of fracture toughness at all service temperatures to ensure ‘fail safe’ lifetimes. In general, yield strengths, Young’s modulus, and tensile strengths increase as the exposed temperature is decreased. The effect of low-temperature exposure on ductility and toughness is, however, dependent on alloy composition, and for specific alloy data special handbooks should be consulted (Campbell 1980; Reed and Clark 1983).

(f) Corrosion

It should be emphasized that several effects of the space environments are beneficial to metallic materials. Before launch many criteria have to be set forth for the selection of spacecraft materials, so that failure resulting from corrosion and particularly stress-corrosion cracking will be prevented.

With the exception of pressure vessels, plumbing lines, liquid fuel cells, and galvanic battery cells, these problems of corrosion are not evidenced in the vacuum environment of space.

(g) Material fatigue

The low and high cycle fatigue lives of parts fabricated from most steels, aluminium and titanium alloys are impressively extended under vacuum conditions—this is particularly welcome as many spacecraft parts will be subjected to extensive mechanical and thermal fatigue during their operational lives. An analysis of the results from extensive test programmes (Grinberg 1982) strongly indicates that the vacuum environment produces a change in the plastic strain intensity in the near-fatigue crack region of all alloys, and an increase in the plastic zone depth of ductile materials. This results in a decrease in crack propagation rate, due in part to the absence or a considerably reduced effectiveness of oxide or chemisorbed films on fresh crack surfaces.

(h) Spacecraft charging

In orbit or in deep space, spacecraft and space vehicles can develop an electric potential up to tens of thousands of volts relative to the ambient extraterrestrial plasma (the solar wind). These large potential differences (called ‘differential charging’) can also occur on the external surface of a launch vehicle. The main consequences of spacecraft differential charging are the phenomena of electrical discharge (‘corona’—which produces a damaging glow around conducting materials at high potential) and arcing (a luminous bridge formed by discharge between spacecraft electrical conductors). Similar discharges may also be observed when high-voltage equipment, such as travelling wave tubes and electronic power supplies, operates on board for the transmission of signals from the spacecraft back to Earth. Many factors contribute to spacecraft charging, including the spacecraft configuration, its structural and surface materials, how correctly these materials are grounded, whether the craft is operating in sunlight or shadow, its altitude above Earth, and the flux density of high-energy solar particles or level of magnetic storm activity. Many possibilities exist to neutralize the spacecraft potential: where possible all interconnecting parts, particularly at the surface, should be electrically grounded to ensure sufficient electrical conductivity between interfaces. This will include solar cell cover glasses and optical solar reflectors (see Sect. 5.5.4). Alternatively, new methods that reduce surface potentials (particularly for scientific spacecraft designed to measure plasma and electric fields in the space environment) are active systems that release a sufficient amount of charged particles across the external surfaces. These particles are ions, emitted

by field emission from a liquid metal source that can be indium. Ion release is usually for a short time, until the spacecraft potential is reduced, or reaches zero.

(i) *Spacecraft in hibernation*

The Rosetta spacecraft was manufactured by a European consortium during the 1998–2003 time period. It was launched in March 2004 with the objective of making a rendezvous with the comet Churyumov-Gerasimenko, otherwise known as 67P. This craft achieved a new “first” in human history, by reaching its destination in August 2014 and began orbiting 100 km above the surface of the icy comet, taking images and then descending to a height of 30 km before detaching its lander, named Philae. Much of Rosetta’s 10 year journey was in hibernation mode. The journey covered 6.4 bn km through the Solar System (three times around the Earth, once around Mars, once close to Jupiter and five times around the Sun). Consequently this spacecraft’s hardware was subjected to most of the space environments compiled into (b) to (h) above. Close to the Sun the problem of overheating was solved by using radiators to dissipate heat into Space. Conversely, close to Jupiter, the hardware and experiments (20 in all) were kept warm by multi-layer insulation blankets and heaters located at strategic points such as fuel tanks, pipework and thrusters. The Philae lander was separated from Rosetta by means of a small pyro (explosive) cable cutter which activated the release of a large compressed spring. Much metallurgical work was conducted prior to launch to ensure that the Carpenter spring steel would not become embrittled at the very low (−160 °C) outer Solar System temperatures, or become cold welded to its mated structural surfaces, during its passage close to the Sun. Philae’s landing gear was also materially demanding due to the low temperatures encountered and low power budget (Thiel et al. 2003). The main components being harpoons to anchor to the comet’s surface: a copper beryllium projectile, pyrotechnic expansion system, cable magazine and a rewind system (AA 7075-T7351) driven by a brushless motor having plain bearings machined from MoS₂-filled polyimide (Vespel SP3).

Rosetta is supplied by power from two 14-m-long solar arrays having a total area of 64 m². The Si solar cells used are 200 μm thick, of low intensity, low temperature type, approximately 38 × 62 mm size. The cover glasses are 100 μm thick ceria doped micro-sheets. Four 10 Ah NiCd batteries store the power to supply the 28 V bus lines.

Many other scientific spacecraft covering great distances use power from radioisotope thermoelectric generators (RTG). For instance, the New Horizons spacecraft, launched in January 2006 has been in hibernation for two thirds of its flight time, and will reach Pluto in mid-2015. On reaching

the most outer bodies known to orbit the Sun, the RGA power system will be turned on and seven science instruments activated.

2.4 Materials for Space Launch Vehicles

At present the only way that satellites, people, and cargo can be carried off from the Earth into the environment of space is by the use of rocket-propelled vehicles. Expendable launch vehicles (ELVs) are used only once. Many nations are involved with the construction and launch of ELVs. The most well known of the several hundred launch vehicles to have boosted spacecraft from Earth are listed in Table 2.6.

The first European telecommunications satellite (OTS) was lost when its ELV exploded during launch, probably due to a defective solid rocket motor case. The failure review established that the steel case material had been incorrectly heat-treated. Parts of the exploded case were retrieved from the Atlantic Ocean by submarine. Metallographic evidence determined that the large cylindrical piece-parts had received an austenitizing time or temperature which was insufficient to solution treat the AISI 4130 (0.3C, 0.95Cr, 0.2Mo rem. Fe) steel. This was apparent from the presence of large-sized spherical carbides in the microstructure of the solid rocket motor case. The flight hardware case had not achieved peak hardness during subsequent quenching and normalizing. Incidentally, the in-line process control sample that had accompanied the flight case did have adequate mechanical and microstructural properties—this was because of the small mass of the test piece which responded well to the time-temperature profile. A replacement spacecraft, OTS 2, was launched successfully 8 months later in 1978 on Thor Delta number 141—this event can be seen in Fig. 2.2. The Delta ELV continues to be one of the most successful US launchers.

A schematic diagram of the main features of a typical ELV is shown in Fig. 2.6. This shows the Titan rocket which was initially developed in the USA during the 1950s and continues to be launched today as a stretched version (Titan in and IV). This ELV, together with the Delta rocket, was complementary to the Space Shuttle fleet, particularly for the launch of heavy payloads. The fleet of Space Shuttles were retired in 2011 and NASA has selected two spacecraft to potentially replace the shuttles. It is intended that the US will take astronauts to the International Space Station (ISS) in 2017 by means of reusable capsules, the SpaceX Dragon and Boeing’s CST-100. Each capsule can be placed on single-use rockets, such as the Falcon 9 Heavy or Atlas 5 series, and they have been designed to carry up to seven astronauts at once. At the time of writing, only Russia is able to transport astronauts to and from the ISS by means of its

Table 2.6 Selected launch vehicles

Country of origin	Launch vehicle (latest known version)	Type ^a	Payload into GTO ^b (kg)
China	Long March 3 (1992)	ELV	2500
	Long March 3B (2007)	ELV	11,500 (LEO)
			5500
European Space Agency	Ariane 4 (1990)	ELV	2600
	Ariane 5 (1996)	ELV	6800
	Ariane 5 (2014)	ELV	10,500
	Vega—Italy (2014)	ELV	1500 (LEO)
India	Vehicle 3 (1979)	ELV	40 (LEO)
	Polar Satellite Launch Vehicle (2014)	ELV	3250 (LEO)
Israel	Shavit (1988)	ELV	160 (LEO)
Japan	H-1 (1986)	ELV	1100
	H-IIB (2009)	ELV	16,500 (LEO)
			8000
USA	Scout (1979)	ELV	5400
	Atlas 2 (1991)	ELV	2700
	Atlas 531 (2014)	ELV	17,000 (LEO)
	Thor Delta (1992)	ELV	2000
	Delta 2 (2012)	ELV	2500
	Saturn V	ELV	10,000
	Titan III and IV (1989)	ELV	5000
	Falcon 9 (2014)	ELV	13,150 (LEO)
	Space Shuttle (1990, <i>retired</i> 2011)	AV	25,000 (LEO)
Former USSR	Vostok (1960)	ELV	5000 (LEO)
	Proton (1968) Russia	ELV	5500
	Soyuz-2.1b (2014) Russia	ELV	3000
	Soyuz-2.1b (2014) Russia	ELV	8500 (LEO)
	Soyuz-2.1v (2013) Russia	ELV	2800
	Zenit 3SL (2002) Ukraine	ELV	6000
	Buran <i>Retired</i>	AV	30,000 (LEO)

Key

^aELV expendable launch vehicle; AV aerospace vehicle

^bGeosynchronous transfer orbit [flight performance to Low Earth Orbit (LEO) is usually more than twice this payload weight]

Soyuz rocket. Supplies of equipment and food are transported to the ISS using either the Russian Progress spacecraft of the European Automatic Transfer Vehicle. Since its first flight in 2008, the ATV has played a vital role in ISS logistics serving as a cargo carrier, ‘space tug’ and storage facility. ATV will evolve into the European Service Module (ESV) designed to support the NASA Orion spacecraft. The deep-space missions envisaged by NASA will rely on the Orion spacecraft—it has been flown on a successful test flight aboard a Delta 4 Heavy booster launched from the Kennedy Space Centre at the end of 2014.

Propellants for launch vehicles are regarded as materials. All rockets are propelled into the vacuum of space by

utilizing only the liquid or solid materials on-board; at present, there is no possibility of using atmospheric oxygen. The term ‘propellant’ is used to denote the two chemical products, the ‘oxidizer’ and the ‘fuel’, contained inside conventional rockets. The fuel is burnt with the oxidizer in order to achieve the enormous amounts of energy needed for liftoff. The propellants can be in either liquid or solid state. Modern rockets are powered by ‘cryogenic’ propellants: liquids which at atmospheric pressure have boiling points below 0 °C. Examples are liquid oxygen (−183 °C) and liquid hydrogen (−253 °C).

The most simple solid propellant is prepared from a mixture of nitrocellulose and nitroglycerine—this is the fuel.

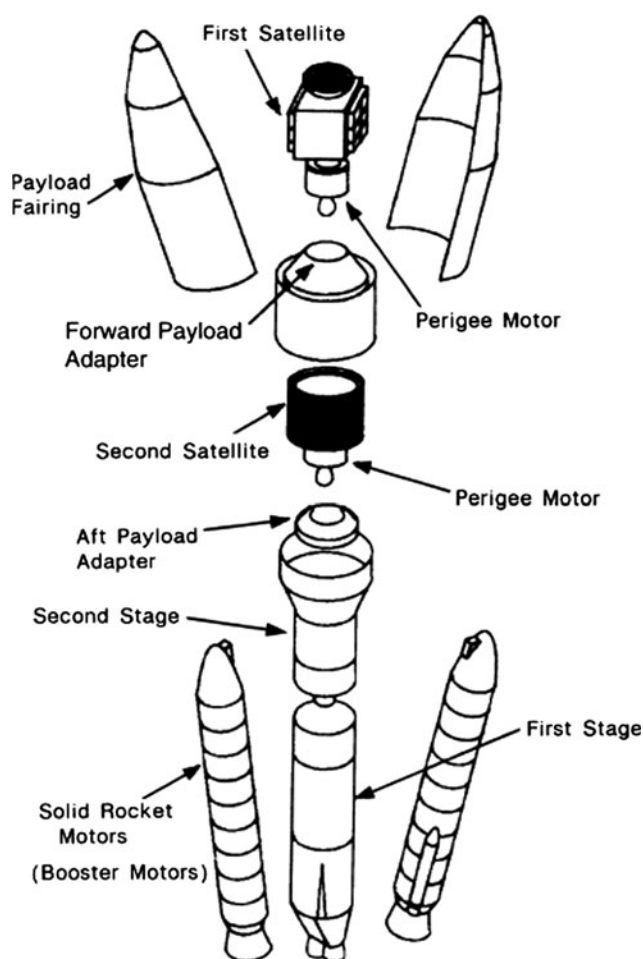


Fig. 2.6 View of the main structural parts of an ELV (based on a Titan III design)

The oxidizer is prepared separately from either ammonium nitrate, ammonium perchlorate, or potassium perchlorate. The fuel and oxidizer are made into powder form and then mixed with binder such as polyvinyl chloride or a polyurethane. The resulting substance is poured into the solid rocket motor casing, where it sets hard. The case is usually made of steel, as discussed previously for the Thor Delta solid rocket motor, but composite materials based on graphite fibres are also used. More complex solid propellant chemistry is based on polybutadiene acrylonitrile (PBAN) and hydroxytelechelic polybutadiene (HTPB) propellant. The HTPB propellant for Ariane V solid boosters is, typically, 68 % ammonium perchlorate, 14 % polybutadiene, and 18 % aluminium powder. Much progress has been made during the last decade in the development of improved solid propellants. One propellant is identified as GAP/Al/HNF [glycidyl azide polymer being the binder, aluminium powder and a new form of powerful oxidizer with the chemical composition of hydrazinium nitroformate (Schoyer 1996)].

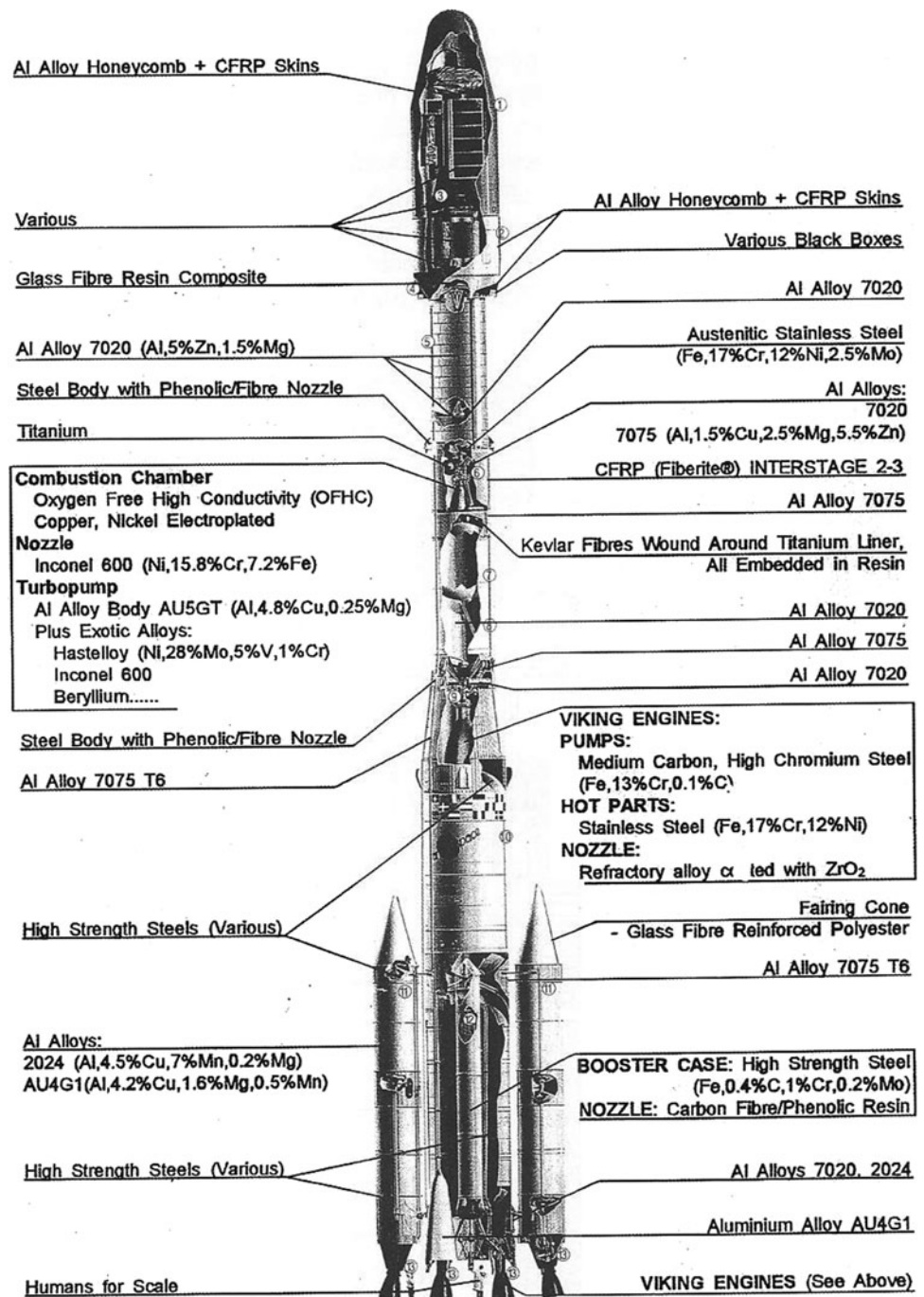
Comparative tests were made between this new propellant and the best-performing HTPB-containing propellant. The findings included an increase in characteristic velocity of about 8 % and, importantly, an ecologically benign exhaust, free of chlorine, where the combustion products are nitrogen, water, carbon dioxide, nitrogen oxide, and aluminium oxide.

Liquid propellant motors are usually fed from two tanks, one containing the liquid fuel (such as kerosene, liquid hydrogen, or hydrazine (N_2H_4)), the other containing the oxidizer (usually liquid oxygen or nitrogen tetroxide (N_2O_4)). Infrequently, fuming red nitric acid or nitrogen peroxide is used. The propellants are injected into the rocket motor's combustion chamber, where ignition and combustion occur with a great release of thermal energy. The combustion gases are then forced through the exit nozzle of the motor. Here, the kinetic energy is absorbed by the nozzle as the gas velocity increases and then decreases through the 'throat' of the nozzle. A drawing of the Ariane IV launcher vehicle parts is shown in Fig. 2.7. The first two stages of this ELV use hydrazine and nitrogen tetroxide. The third stage is propelled by a cryogenic engine fed by liquid hydrogen and liquid oxygen. As illustrated in the figure, Ariane IV has the possibility to incorporate either liquid or solid propellant booster motors to assist in the first stage liftoff.

In contrast to Ariane, the Space Shuttle was, as its name implied, reusable and of extreme importance for its role in manned, near-Earth activities. The Shuttle's primary propulsion consisted of a large external tank (47 m in length and 8.7 m in diameter) which contained compartments for the liquid oxygen/liquid hydrogen propellants—these were fed to the three main engines, and two strap-on booster motors which contained a solid composite propellant (polybutadiene, acrylic binder, and ammonium perchlorate oxidizer).

Rocket structural materials are usually based on the Duralumin series of aluminium alloys (4 %Cu, 2 %Mn, rem. Al). These alloys have high strength-to-weight ratios and are detailed in further sections of this book. Concerning Ariane IV, much use has been made of the aluminium alloys AU4GN (AA2024), AZ5GU (AA7075), and AZ5G (AA7020). These are the French alloy designations with the US Aluminium Association designation in parentheses. Further cross-references to national alloy specifications are given in Appendix 6. Some locations for these alloys are indicated on Fig. 2.7. Unfortunately, several of their heat-treatment conditions are susceptible to stress corrosion cracking (SCC). A particular problem resulting from SCC is discussed in Sect. 4.5. All the major structural materials used for the construction of Ariane and its motors are identified in Fig. 2.7. The more modern rocket motor and booster bodies containing solid propellants are machined and welded from 'maraging' steels, which are based on iron with large amounts of nickel, cobalt, and molybdenum. These steels

Fig. 2.7 Launch vehicle inbound profile with main structural materials indicated (Ariane IV, 42 LP)



can be easily rolled and formed into complicated shapes, then welded—after this a suitable heat treatment is made which produces very hard and tough material properties.

Liquid fuels and oxidizers are usually stored in pressure tanks which may be made of titanium or aluminium alloys, as shown in Fig. 2.8. These inner surfaces which make contact with the liquid fuels must be tested and found compatible and non-igniting with the liquid. For instance, the titanium alloy Ti6Al4V is known to be compatible with hydrazine, and aluminium alloys compatible with liquid

oxygen. Similarly, any pressure vessel liner materials based on organic materials need to be compatibility tested—this is more difficult, only one resin system, Torlon AI-10, being found to be compatible with liquid oxygen (Healy et al. 1995).

The Zenit ELV of the former Soviet space agency was formally announced in 1989. The vehicle is a two-stage liquid oxygen and kerosene rocket which, like all CIS launchers, is assembled horizontally. Its launcher assembly, payload integration, and launch preparation phases have

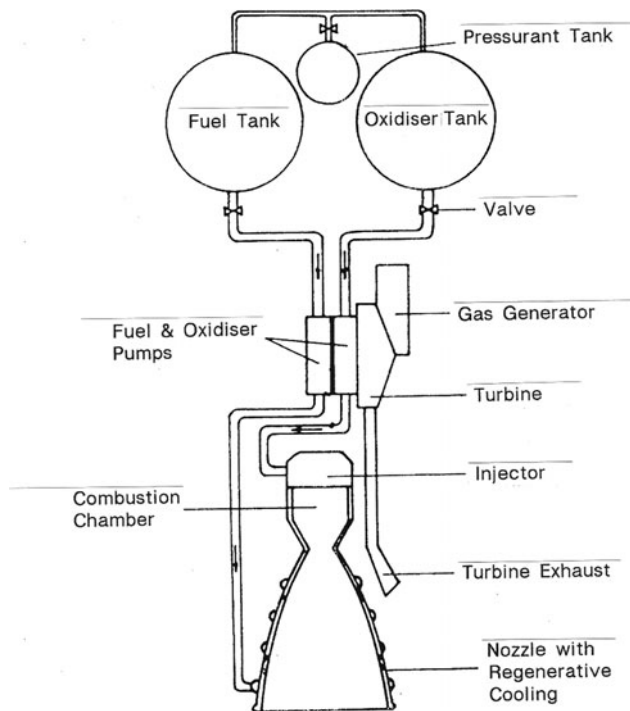


Fig. 2.8 A liquid propellant rocket engine

been described as ‘highly automated’ (Isakowitz 1995). General views of the Zenit assembly hall and its kerosene–LOX engine are seen in Figs. 2.9 and 2.10 respectively. This ELV has recently been proposed for launching satellites from the sea. The novel idea is to utilize a covered semi-submersible oil rig as the firing platform. This would be anchored in the Pacific, at the Equator, so making full advantage of the Earth’s maximum rotational velocity (about 1600 kph). The Zenit rocket, standing 62 m tall, would face eastward in a direction avoiding any inhabitable landfall. All other major world space launch sites are rather far north from the Equator with the exception of ESA’s facility at Kourou, French Guiana, which is less than 500 km north of the Equator. The uniquely flexible ‘Sea Launch’ site will undoubtedly require the implementation of a comprehensive corrosion protection scheme for all the associated spacecraft materials.

The Ariane V development was initiated by the European Space Agency in 1985. It is designed for commercial missions to launch satellites and cargo for the future space stations. The proposal for launch of the European Hermes as a reusable winged manned space vehicle atop the Ariane V was cancelled in the mid 90’s. However, it has flown several cargo vehicle [Automated Transfer Vehicle (ATV)] and is designed for a Crew Transfer Vehicle (CTV). An illustration of the Ariane V in a dual launch configuration is shown in Fig. 2.11. Ariane V has a length of 54 m, a gross mass of 710,000 kg, and a designed thrust at liftoff of 15.9 MN. The

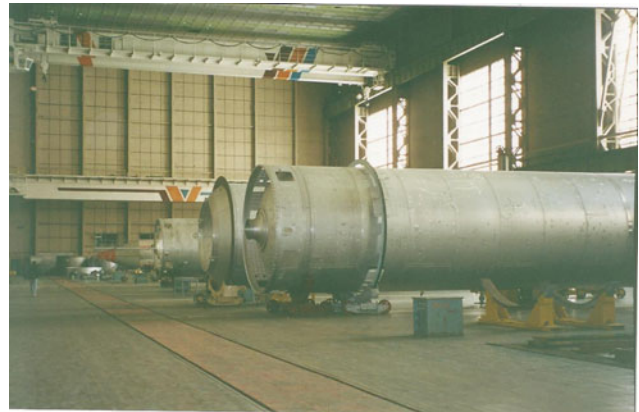


Fig. 2.9 General view of the Zenit assembly hall



Fig. 2.10 Installation of Zenit first stage kerosene–LO₂ engine

Vulcan engine powers the Ariane V main cryogenic stage. This engine consists of a gas generator cycle, in which turbopumps driven by a gas generator fed by propellants tapped from the main supply system feed fuel and oxidizer to the combustion chamber. Liquid oxygen (oxidizer) and liquid hydrogen (fuel) are sprayed into the combustion chamber. Because of the extremely high combustion temperature, reaching 3600 °C and with about 1600 °C at the internal wall of the chamber, it is necessary to cool the chamber. This is done by machining channels into the chamber wall—there are 360—and passing liquid hydrogen through them as the engine is fired. The chamber is fabricated from a wrought high-strength copper alloy (Narloy-Z) with an outer band of nickel. The combustion chambers of the Space Shuttle main engines were also made from Narloy-Z (Cu, 3Ag, 0.5Zr wt% with O₂ of approximately 50 ppm) and, when correctly heat treated, this alloy was ideal for combustion chambers operating from –252 to 540 °C but above this temperature the hot wall mechanical properties were degraded because of grain growth, grain boundary sliding and bulging that

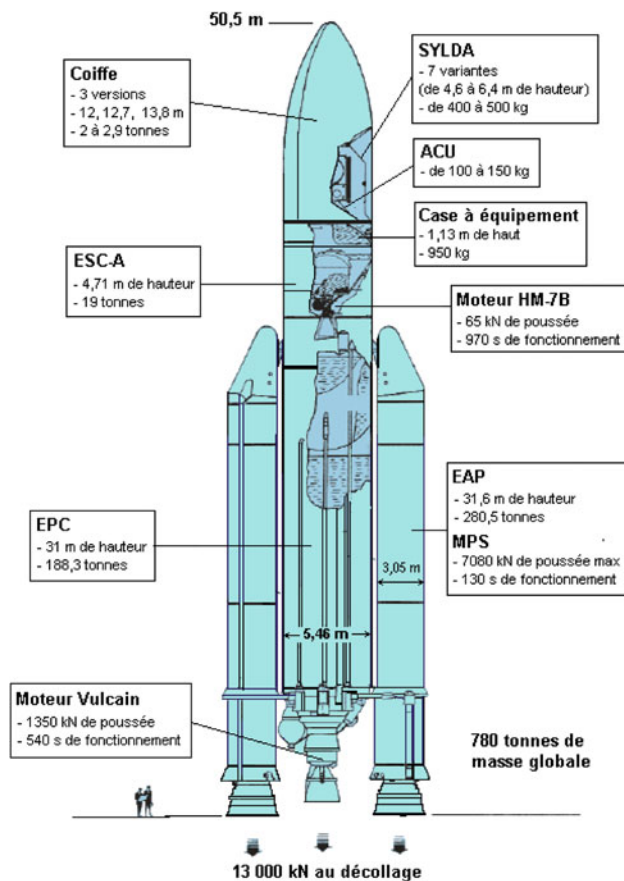


Fig. 2.11 The main system of Ariane 5. *Note* For Ariane 5, all the welded aluminium AZ5G (AA 7020) alloy previously selected for the structure of Ariane 4, has been replaced with AA2219 owing to this alloy's improved resistance to stress corrosion cracking. The painted surfaces of Ariane 5 can be seen in Fig. 4.113

resulted in cracking (Singh 2005). The liquid hydrogen passing through the coolant passages at $-252\text{ }^{\circ}\text{C}$ not only cools the chamber and prevents the Narloy Z from melting, but it is itself heated, and in turn injected into the combustion chamber. A cross-sectional view of the chamber wall is shown in Fig. 2.12 and is described in its caption. The Vulcain engine develops 1.12 MN of thrust by ejecting some 250 kg s^{-1} of gases at very high speed. These gases—harmless to the environment as they are basically water vapour—are accelerated by the nozzle to a supersonic speed. Like the combustion chamber, the bell-shaped nozzle is also cooled by a flow of hydrogen. Hundreds of test firings have been made with many Vulcain engines in order to demonstrate that the engine meets its performance specifications. Some firings (see Fig. 2.13) have exceeded 18,000 s of operation so that engine material and equipment limits (endurance, failure modes, etc.) can be determined. It is here that work involving metallurgical inspections and detailed failure evaluations is important—the reporting of these tasks

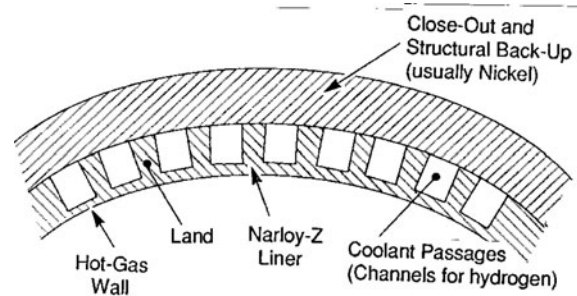


Fig. 2.12 Cross-sectional view of combustion chamber wall showing the rectangular coolant channels machined into the chamber lining (Narloy-Z, a copper-silver-zirconium alloy with significantly greater strength than pure copper but with only slightly lower thermal conductivity). The close-out band is made of thin electroplated copper followed by electroplated nickel. This design is incorporated in the Space Shuttle main engine and the Ariane HM60 and Vulcain engines

forms part of the quality assessments and assists in the generation of reliability ratings.

An interesting new development is the 3D printing of a full size combustion chamber by engineers at NASA-MSFC. The cooling channels, similar to those seen in Fig. 2.12, consist of 200 intricate conduits with complex internal geometries. They are located between the inner and outer liner walls and although difficult to accommodate, were successfully built in by additive manufacturing. The copper alloy powder used for the 3D printing is GRCo-84, a material developed by NASA Glen Research Centre. It has been stated (Hipolite 2015) that the selective laser melting machine at MSFC fused 8255 layers of the alloy powder to make the chamber in under 11 days.

Whereas the main structural alloy for the Ariane IV launcher was aluminium alloy AZ5G (AA7020), a major decision was made during the design stage of Ariane V to change to the alloy AU6MT (AA2219) as shown in Fig. 2.11. The liquid oxygen (LOX) tank of the main cryogenic stage is made from two hemispherical sub-assemblies machined from AA2219 dye forging. An equatorial weld unites these parts. During the ground-hold period just prior to launch of Ariane V the LOX tank is pressurized with helium, initially loaded into the tank as liquid helium. An internal pressure of 21–23 bar is maintained during the flight of Ariane V. This high pressure and the operation of the LOX tank at cryogenic temperatures under the enormous vibrational and flight loads, requires that the AA2219 material and its weldments are extremely well controlled by metallurgical techniques.

As a further example, the Ariane V upper stage, storable propellant system (EPS), consists of 4 EPS tanks for the storage of N_2O_4 and monomethyl hydrazine. These tanks are also constructed from AA2219 material by direct current,



Fig. 2.13 Test firing of the Vulcain-2 engine (courtesy of SNECMA, France). The nozzle exit diameter is 2.5 m. Liquid hydrogen fuel is used to cool the engine, flowing through a jacket surrounding the thrust chamber. The heat absorbed this way is necessary in prolonged firings and enhances the initial energy content of the LOX and LH2 propellants prior to injection into the combustion chamber where the highly exothermic reaction produces steam ($2\text{H}_2 + \text{O}_2 \rightarrow 2\text{H}_2\text{O}$) and more than 1000 kN of thrust. The nozzle supports rectangular tubes made from Inconel[®] and welded together to form a helical structure through which the hydrogen coolant flows (Suslov et al. 2010)

variable-pulse TIG welding. They have a volume of 2335 l each, made up from two spin-formed hemispheres and an equatorial ring. The initial 2219 is procured as sheet in temper '0'. A blank is precontoured on a lathe and this is convex spin-formed in 21 steps at a temperature of 200 °C. The alloy is then solution heat-treated and quenched (535 °C for 50 min, then water-quenched within 10 s). The parts are then stretched by 1–3 %, which results in the temper 'T-31'. The parts are welded and subsequently warm-aged at 177 °C for 18 h in order to achieve high strength properties. Metallurgical assessments are made throughout these process steps in order to control against grain coarsening of the 2219. Heating temperatures for spin-forming must not be so high as to induce grain growth. Also, strain-hardening steps

have had to be optimized in order to achieve the tanks' required margin of safety.

The large-diameter Ariane V solid propellant booster motor cases (EAP) are seen in Fig. 2.11. These are thin-walled tubes formed by the novel process of 'counter-roller flow forming'. The material is the steel 48CDNV4 (American D6AC), for which a large amount of thermomechanical processing and property data are available. Conventional tube spinning is to place a cylindrical tube blank on a solid cylinder mandrel and roll the outer surface of the tube so that it becomes thinner and longer. The special flow-forming process applied by the German MAN company is to place a cylindrical blank tube of D6AC between four roller-pairs. The roller-pairs are separated by a fixed distance that will be the final tube diameter. The tube is initially attached to a face plate, which can rotate. The tube wall thickness is forced into each roller-pair. As the tube is rotated, the roller-pairs are fed down the length of the tube, causing it to elongate and become thinner. Metallurgical assessments making use of mechanical testing and metallography were used during this process development in order to optimize the flow compression stresses in the deformation zone and understand their effects on the steel's micro-structure. The motor thrust frame on the main stage of Ariane 5 is essentially an unpressurised conical structure consisting of many integrally machined parts made from AA 7075. These are mainly interlocked by manually installed Hi-lok[™] fasteners, but these lap-joined parts have also been proven to be reliable when joined by friction stir welding (FSW) methods (Brooker 2001).

Several companies are considering designs and the use of new materials for future reusable launch vehicles. Single stage to orbit (SSTO) launch systems will use advanced metallics and advanced composite materials, and it is the re-entry phase for such craft which will generate the highest aerodynamic heating rates. In the early 1970s many data had been established for a wide range of quality refractory metals based on molybdenum and molybdenum–rhenium alloys that were covered with protective coatings. These heavy alloys were abandoned in the mid-1970s once NASA had decided to select a ceramic reusable material for the thermal protection of the Space Shuttle.

There are several kinds of heat shield. The system designed for the Shuttle is the most advanced to have flow to date. On the Mercury, Gemini, and Apollo capsules, the shield consisted of an epoxy-resin compound that removed heat by flaking off as it passed through the atmosphere. This kind of 'ablative shield' can be used only once. The newer thermal protection material was developed by NASA's Ames Research Laboratory and the Lockheed Missiles and Space Company. It is very lightweight, relatively easy to manufacture into small square tiles, and impervious to heat (one

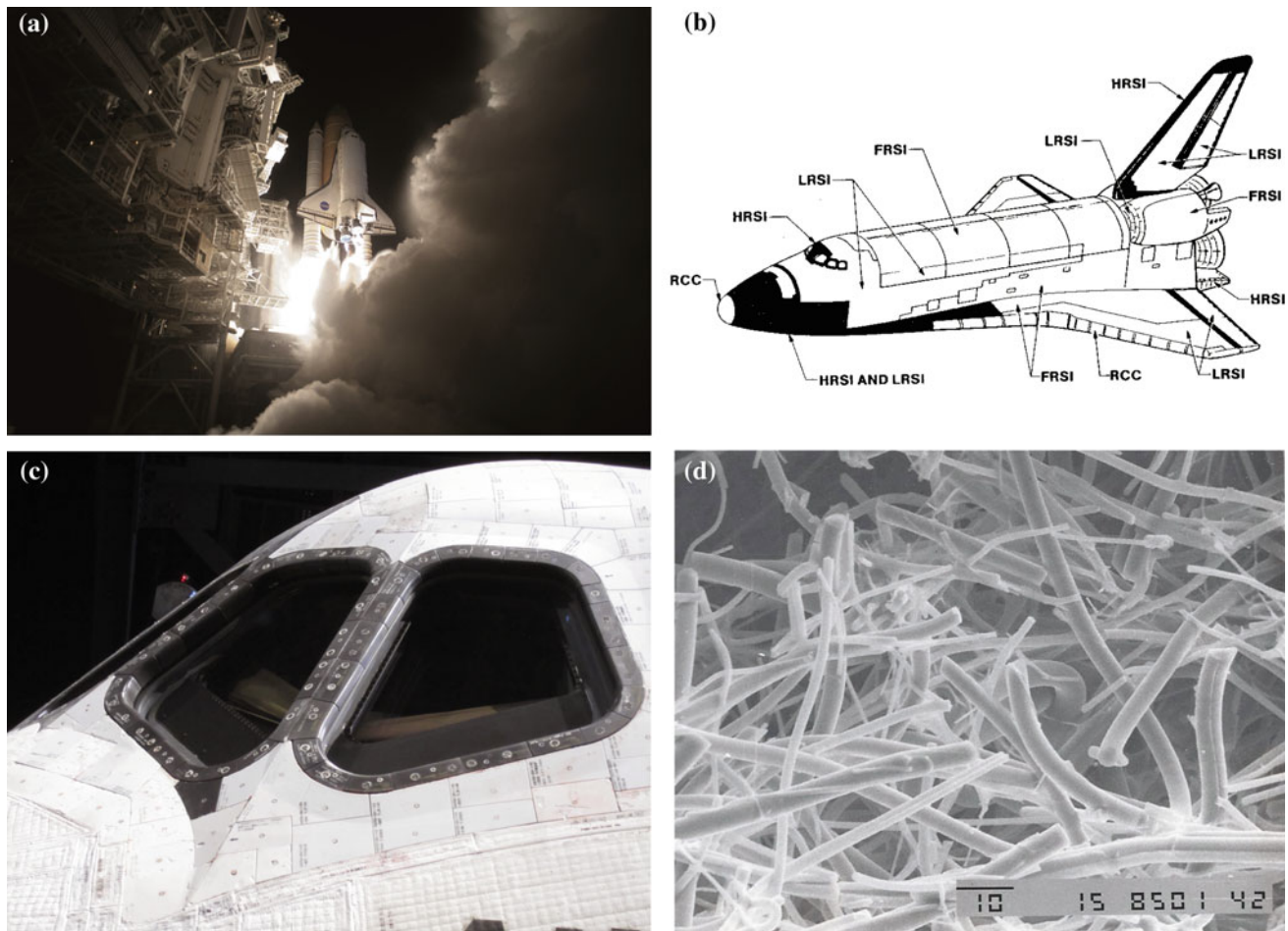


Fig. 2.14 **a** Night launch of Space Shuttle. **b** Illustration of the thermal protection systems (TPS) for the Space Shuttle fleet. **Key:** RCC reinforced carbon/carbon; HRSI and LRSI high- and low-temperature ceramic tiles; FRSI felt reusable surface insulation. **c** Atlantis

photographed at the KSC Visitors Centre after retirement; showing the triple paned, optical quality windows, the LRSI ceramic tiles and beryllium is associated with the window frames. **d** Scanning electron image of Shuttle tile (silica fibers in unglazed condition) $\times 1000$

can hold a six-inch square tile at its edges and not feel any heat when the centre of the tile is glowing red-hot). There are about 31,000 tiles on each Shuttle, each moulded and cut to fit the orbiter's contours. The basic material for the Shuttle insulation is a very fine glassy fibre of pure silica (SiO_2). Figure 2.14a shows the approximate layout of the various Shuttle thermal protection systems (TPSs). The reinforced carbon-carbon (RCC) regions can reach temperatures of up to 1500°C during descent through the atmosphere. The reusable felt surface insulation may reach 500°C during ascent. The HRSI and LRSI ceramic tiles differ only in their surface coatings (Vaughn 1985). The high-temperature (HRSI) tiles are coated with a high-emissivity black reaction cured borosilicate glass (to re-radiate the heat efficiently during re-entry). The low-temperature material is coated with a white silica/alumina coating designed to reflect the sun's radiation as the craft is in orbit. Figure 2.14b shows the microstructure of a ceramic tile's interior. Here, the fibres are

seen to vary in diameter from 1 to $10\ \mu\text{m}$. This material has a density of $136\ \text{kg m}^{-3}$, but more rugged varieties are denser and some contain boron, which causes the fibres to weld together. The thermal protection surfaces developed from Shuttle experience are now very robust. The alumina-enhanced thermal barrier tiles overcoated with reacting cured glass have been produced that can withstand the impact of 800 kph raindrops (Healy et al. 1995). The tiles are bonded onto the aluminium skin of the Shuttle with a silicone adhesive known as RTV 560, which is a somewhat soft material that avoids cracking of the rigid tiles as the aluminium airframe deflects in flight. Thermal protection is not needed for lower surface temperatures; for instance, Inco-617 could be selected for temperatures under 980°C and Ti-1100 for temperatures below 700°C (Baumgartner and Elvin 1995).

The retirement of the Shuttle fleet in 2011 has meant that crew members from the ISS can only return to Earth by



Fig. 2.15 Engineers completing the installation of the heat shield on NASA's Orion spacecraft. The Avcoat ablative material is covered with a silver reflective tape that protects it from the extreme cold temperatures of space. The heat shield has been shown able to protect the Orion crew from temperatures in the order of 2800 °C during re-entry and ocean splashdown (courtesy NASA)

means of the Russian Soyuz Descent Module. This vehicle can hold up to three astronauts/cosmonauts and takes about 3.5 h to return and land on the flat grassy plains of Kazakhstan in central Asia. Four parachutes dramatically reduce the speed of descent 15 min before landing, followed by the final main parachute which reduces the speed of the craft to 24 feet per second and at this speed, one second before touchdown, the vehicle is slowed down to make a soft landing by the firing of two small engines located at the bottom of the vehicle.

NASA's Orion crew module (Fig. 2.15) is designed to accomplish manned missions to the Moon, an asteroid and even Mars. On its return to Earth this spacecraft will descend through our atmosphere much like the Apollo capsules. The first Orion was launched in December 2014 atop a Delta 4 Heavy rocket in a test flight to check many of the systems critical to safety. It has shown that advances in heat-shield design and materials technology can tolerate temperatures in the order of 2800 °C during decent phases of such missions. The Orion heat shield consists of a titanium skeleton covered with a carbon-fibre skin. This skin is later covered with a honeycomb layer composed of fiber-glass and phenolic resin. The honeycomb cells are then filled using a hand-held dispensing gun with a material called Avcoat, a mid-density ablator that is similar to the ablative material used on the Apollo command module (Reuther 2010). Avcoat is an epoxy novolac resin, designated by NASA as 5026-39-HC/G (with a revised composition that contains less carcinogenic compounds than the Apollo shield chemistry).

The Falcon 9 rocket is an evolved expendable two-stage launch vehicle manufactured in the US by the SpaceX company. It made history in 2012 by launching the Dragon spacecraft (somewhat similar to Orion) into the correct orbit

for rendezvous with ISS. Falcon 9 has nine first-stage engines and a single second stage engine, this configuration is considered to reduce the number of possible separation "events". Falcon 9's faring is manufactures in two halves from sheet carbon fibre bonded to an aluminium honeycomb core. The first stage tank is manufactured from aluminium-lithium alloy by means of friction stir welding and it contains two aluminium tanks that are capped by aluminium half-domes for the liquid oxygen and RP-1 propellant respectively. The second stage is manufactured similarly to the first stage from Al-Li and the interstage utilizes a composite structure made from carbon-fibre lay-uped onto an aluminium core. Unusually, a pneumatic separation is employed for the faring and for both interstage separations, in order to reduce the shock forces that accompany the firing of pyrotechnic devices. The follow-on Falcon Heavy, presently in design phases, is expected to be the most powerful rocket flying—only the Saturn V moon rocket last flown in 1973 could deliver more payload into space.

A recent addition to the European family of launchers is Vega (see Fig. 2.16) developed initially by the Italian Space Agency (ASI) and Italian industry (see Table 2.6). Vega became officially an ESA programme in 1989 and the first Vega lifted off from the Guiana spaceport in 2012 on a flawless qualification flight. The three subsequent launches were fully successful and nine further launches are planned post-2015.

A breakdown of the advanced materials used to construct Vega (2006, VEGA) can be listed in a similar way to those selected for Ariane and illustrated in Fig. 2.7.

Payload Faring:

Structure comprises of two halves of sandwich panel CFRP sheets and Al honeycomb core that has been already used on Ariane 4.

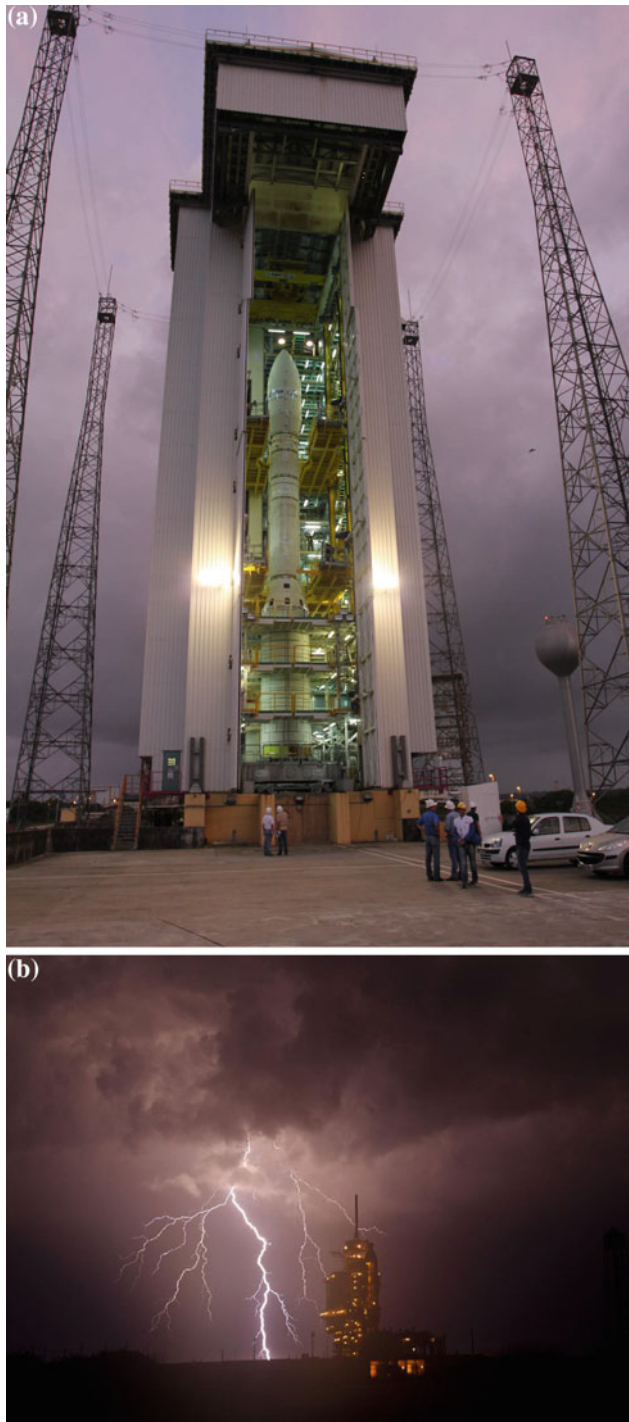
AVUM liquid rocket (UDMH and nitrogen tetroxide) Upper Stage:

Carbon-epoxy cylindrical case with propellant stored in two identical titanium tanks as seen in Fig. 2.17.

First Stage (with solid rocket motor SRM P80FW), Second Stage (with SRM ZEFIRO 23) and Third Stage (with SRM ZEFIRO 9):

Structures are graphite-epoxy filament wound monolithic motor case protected by low-density thermal insulation packed with microspheres (EPDM). The interstages are forged rings of either 7075 or 7175Al alloy in the T7351 heat treatment condition (for each of the 1/2, 2/3 and the 3/Avum interstages) and these are chromic acid anodized for corrosion protection. Some separation springs are made from 17-7PH steel. The solid propellant for the solid rocket motors is monolithic Finoxil grain shaped with a star shape on the nozzle side and EG1LDB3 low-density EPDM based rubber insulant. The motor nozzles are made from: 3-D carbon/carbon throat and carbon phenolic exhaust cones.

In 2015 the Vega rocket successfully launched a 5 m-long wingless reusable spacecraft, weighing 2 t, into a suborbital



◀ **Fig. 2.16** **a** Evening view of a mock-up Vega launch vehicle within the mobile gantry in Kourou. Vega benefits from the location of the European Spaceport, GSC, at Kourou in French Guiana as it lies close to the Equator. The vehicle will take small payloads into a variety of orbits including Low Earth, Sun Synchronous and Polar. Note the four tall lightning rod towers stretching far above the mobile gantry and the housed launch vehicle. Lightning is very common at both KSC and GSC sites so it is important that launch vehicles are protected against the ionized plasma that constitute the branches of lightening discharges. The tops of four towers are interconnected by stainless steel catenary cables which form effective Faraday shielding. **b** Kennedy Space Center in Cape Canaveral, Florida. Space shuttle Endeavour sits on Launch Pad 39A as a storm passed prior to the rollback of the Rotating Service Structure on 28th April 2011. The fixed service structure (FSS) seen here, is 106 m high to the top of its lightning mast. The following day Endeavour launched the STS-134 mission to deliver a high pressure gas tank, spectrometers, spare parts and antennae to the ISS. 39A has been used for the manned Apollo-Saturn V launches. SpaceX, the new commercial space company now launches its Falcon 9 and Falcon Heavy from this same pad

be the effect of the flight profile on IMV's structural materials and the hypersonic aerothermodynamics phenomena whereby air (O_2 and N_2) molecules are dissociated at high velocities and temperatures. A wide variety of materials are being tested during the IMV test flights into low Earth orbit. These include different types of ceramic matrix composites used on the nose, hinges and flaps and ablative thermal protection materials such as Portuguese cork and silicon-based materials to withstand the severe re-entry environment up to 1700 °C.

Silicon carbide fibre reinforced metal matrix composites are of increasing interest for aerospace and space applications. The surge in interest in the late 1980s was driven by interest in the USA and Europe in hypersonic vehicles requiring high specific strength and stiffness materials with elevated temperature capability. Further aerospace work has focused on actuators and landing gear where the very high compressive strength (2.5–4 GPa) coupled with low mass and corrosion resistance make them ideally suited to replace steel and other metallic parts with 30–40 % weight reductions typical (Fig. 2.18a). The increased aerospace development has re-established interest from the space sector with the low mass high compression strength and potential for welded joints being of particular interest for space craft structures and robotic systems.

The Reaction Engines Skylon spaceplane has identified titanium MMCs as a suitable material for the fuselage truss structure and other static components (Fig. 2.18b, c). This truss structure needs good tension and compression properties and potential for elevated and cryogenic temperature operation. The truss structure also needs a low mass and easily assembled jointing for the MMC tubes which can be welded and inspected with upwards of 60,000 tubes over the 80 m fuselage. Other materials incorporated into this spaceplane are seen in Fig. 2.18d.

path. The craft, named Immediate Experimental Vehicle (IMV), separated from Vega at a height of 450 km and reached a speed of 7.5 km/s, later demonstrating maneuverability using thrusters and aerodynamic flaps to reduce speed from hypersonic to supersonic. It then glided through the atmosphere before deploying a parachute and landing in the sea—the craft was then picked up by a recovery vessel and shipped to ESA-Estec for analysis. Of key concern will

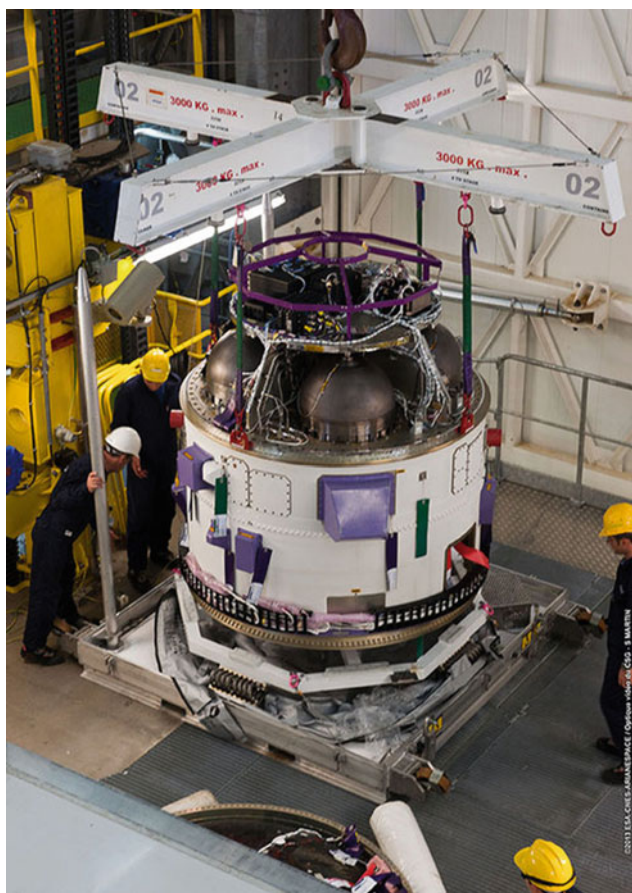


Fig. 2.17 Installation of the final stage of the second Vega (VV02) launch vehicle inside the mobile gantry at GSC. This upper stage is called the AVUM (Attitude Vernier Upper Module) contains the Propulsion Module that burns pressure-fed UDMH and nitrogen tetroxide as propellants (built by the Yuzhnoye Design Bureau) and the Attitude Control System (courtesy ESA)

2.5 Non-metallic Materials

2.5.1 General

Non-metallic materials appear throughout the chapters of this book as they are selected during the design and manufacturing stages of every spacecraft subsystem. Once, only metallic materials, specifically alloys, were used for individual structures, housings and tanks. Nowadays, as the physical and mechanical properties of organic and composite materials have been developed for terrestrial use and refined for the space environment, spacecraft are often constructed from more (both volume and weight) “non-metallics” than metallic materials.

Spacecraft utilize plastics for components, elastomers for propellant diaphragms, lubricants for bearings, polymers for circuit boards and paints, textiles for astronaut’s spacesuits, adhesives for structural bonding, ceramics for optical mirrors

and composite materials for an equally exhaustive list of applications.

Nonmetals are often defined as not containing “metals” and that they are able to combine with hydrogen, carbon and oxygen to form stable compounds. This is a very loose term as most non-metallic materials do contain metallic elements. Polymers and elastomers are formed when monomers and other “-mers” are combined together and this is often referred to as polymerization. These reactions are often not completed and some material remains as an unreacted fragment. Similarly, the reaction may be complete but there remains a byproduct that may be unstable, particular under vacuum. Other polymers or organic materials will often contain deliberate additions of chemicals and metals which impart special properties such as flame retardation, anti-oxidation, colouration, and electrical or magnetic properties.

Sublimation, or the transition of solid metals directly to a gaseous phase (without passing through an intermediate liquid phase) has been discussed in Sect. 2.3b. Certain metals and alloys are specifically forbidden from space use as they can sublime from one surface on the spacecraft and later condense on another, not necessarily cooler, surface to cause problems such as optical degradation of mirrors and electronic short circuits. The behavior of organic materials under vacuum is more complex than that of sublimation. Organic materials are said to “outgas under vacuum”. Here there can be an immediate loss of species such as H_2O , CO_2 and N_2 from a surface, followed by constituents having a low molecular weight, a process akin to distillation. Raising the temperature causes more molecules to outgas and there may be some breakdown of chemical bonds resulting in further outgassing and reduction in weight of the organic material. With time, there can be solid or gaseous diffusion from the material’s interior to the surface and this can cause the material to further degrade in properties or lose weight in a vacuum or space environment.

Outgassing is one of the most problematic behavior of spacecraft materials as the outgassed species can recondense on thermal control surfaces, optical surfaces, electrical contacts (rendering them open-circuits) and cause corona effects. Each of these problems are described as case studies or failure modes within this book and can be located via the Index.

Most of the Space Agencies have performed tests on organic materials during the screening of potential spacecraft materials and their processes. The main test procedures are those defined by the American Society for Testing of Materials (ASTM 2007) and ECSS (ECSS-Q-ST-70-02), these are considered important reading for those involved with material selection. Basically, the test is performed on very accurately pre-weighed samples (between 100 and 300 mg) positioned in a specially designed holder. Each sample is conditioned (24 h at 22 °C at 55 % RH). The

Fig. 2.18 **a** Illustration of a landing gear side stay made from silicon carbide fibre reinforced titanium alloy matrix highlighting its light-weight property. This is 30 % lighter than the forged aluminium baseline. Courtesy of TISICS Ltd., Farnborough. **b** The Skylon spaceplane is unpiloted, reusable and intended to transport up to 15 t of cargo into space. It will use the SABRE engine that combines air-breathing and rocket cycles so that take-off is possible from a runway, flight is direct into Earth orbit and return is, like an aircraft, back to a runway. **c** These Skylon truss struts have been tested in compression up to 50 kN exceeding the 30 kN design load. Actually a couple of struts did fail around 50 kN. In tension they fail close to 30 kN indicating that there is room for further improvement in the 'cuff' region. **d** The materials proposed for construction of Skylon are silicon carbide fibre reinforced titanium for fuselage and wing spars, aluminium alloy for the propellant tank, the external "aeroshell" is made from fibre reinforced ceramic, and the landing gear will possibly use silicon carbide fibre reinforced titanium matrix composite. Courtesy of Reaction Engines Limited

(a)



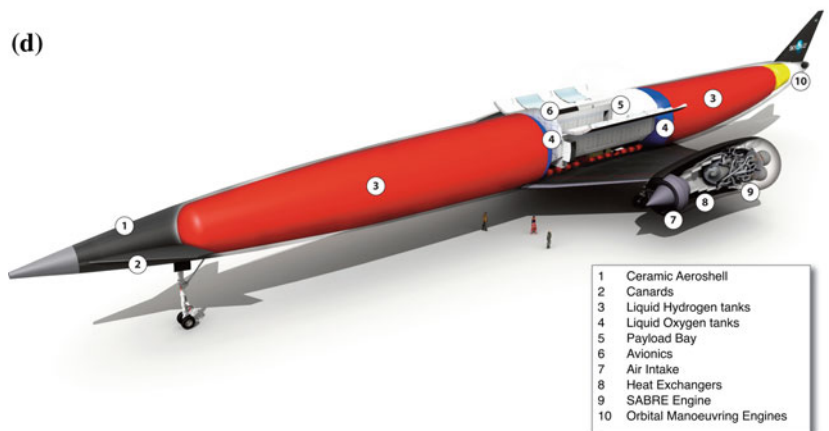
(b)



(c)



(d)



holder is transported into a vacuum chamber having specified dimensions. Testing is made under vacuum at 1 Pa, at a temperature of 120 °C, for 24 h. A collector plate is maintained at 25 °C and situated at 10 mm above the sample during the test period. Figure 2.19 illustrates the basic concept of the outgassing test method. After the sample's temperature/vacuum/time exposure, the sample is again weighed. It is then re-conditioned at 55 %RH (in order to re-absorb any water) and re-weighed. The mass of condensed material on the collector plate is also measured by accurate weighing.

The following terms should be understood:

collected volatile condensable material (CVCM)—quantity of outgassed matter from a test specimen that condenses on a collector maintained at a specific temperature for a specific time

NOTE CVCM is expressed as a percentage of the initial specimen mass and is calculated from the condensate mass determined from the difference in mass of the collector plate before and after the test.

recovered mass loss (RML)—total mass loss of the specimen itself without the absorbed water

NOTE 1 The following equation holds: $RML = TML - WVR$.

NOTE 2 The RML is introduced because water is not always seen as a critical contaminant in spacecraft materials.

The WVR is the water vapour regained by the sample after reconditioning.

total mass loss (TML)—total mass loss of material outgassed from a specimen that is maintained at a specific constant temperature and operating pressure for a specified time

NOTE TML is calculated from the mass of the specimen as measured before and after the test and is expressed as a percentage of the initial specimen mass.

The following Accept Criteria are generally contractual requirements set by the customers procuring space hardware, but it is accepted that many spacecraft units can be baked in order to satisfy these materials requirements:

As a minimum, the outgassing screening parameters for a material selection shall be as follows:

1. $RML < 1.0 \%$;
2. $CVCM < 0.10 \%$.

NOTE 1 For materials used in the fabrication of optical devices, or in their vicinity, the acceptance limits can be more stringent than those stated below.

NOTE 2 It is nowadays becoming standard practice to bake critical hardware (such as structural parts, harness, electronic boxes and thermal blankets) to the highest

permissible temperature for a few days in order to remove residual contaminants, process contaminants and handling contaminants.

Several compilation tables of outgassing data of materials intended for spacecraft use have existed since the 1960's. Of course, much of that data is now obsolete as material manufacturers and suppliers update their products and withdraw some from the market. Importantly, some manufacturers may have retained their product's Trade Name, but changed the procedure by which it is made. This makes it important to check outgassing data on every batch of production—unless safeguards are made to ensure that products conform to certificates of compliance, or that process identification documents (PIDs) are established and audited by the procuring agent.

Websites can be visited to acquire some preliminary data, unfortunately they are often not kept up-to-date, and include:

<http://outgassing.nasa.gov/>

<http://TEERM.nasa.gov/links/html>

http://esmat.esa.int/Services/outgassing_data/outgassing_data.html

Testing for outgassing may be made at centres such as: Integrity Testing Laboratory, Markham, Ontario, Canada; AAC, Wiener Neustadt, Austria; ESA-Estec, Noordwijk, the Netherlands; INTA, Spain; TS-Space Systems, UK, and the Goddard Space Flight Centre, Greenbelt, MA, USA.

Outgassing is distinctly different from the *offgassing* of a material. Outgassing, as previously discussed, occurs under a reduced pressure or vacuum. When materials emit volatile compounds in an ambient atmosphere this is termed offgassing. It can be likened to the smells that are emitted from the interior of a new car. In the 1970's the offgassing of art objects in a museum were investigated and found to be related to the degradation of both antiquities and their packaging materials—a standard “Oddy” test method was devised using gas chromatography-mass spectrometry (GCMS) analysis. Many offgassed species were found to degrade stored antiques, they were based on alcohols, acids, amines and siloxanes (Tsukada 2012). In one specific case, amines were found to volatilise from polyester polyurethane foams that were used to cushion and padding within storage cases. The amines released by these foams had severely damaged Ming Chinese jars by causing thick white efflorescent deposits to form on these ancient pieces. Very similar contamination from offgassed foams has resulted in the corrosion of stored spacecraft electronic components: leads finished with silver, nickel and also tin-lead have become tarnished and sometimes so oxidised that they are

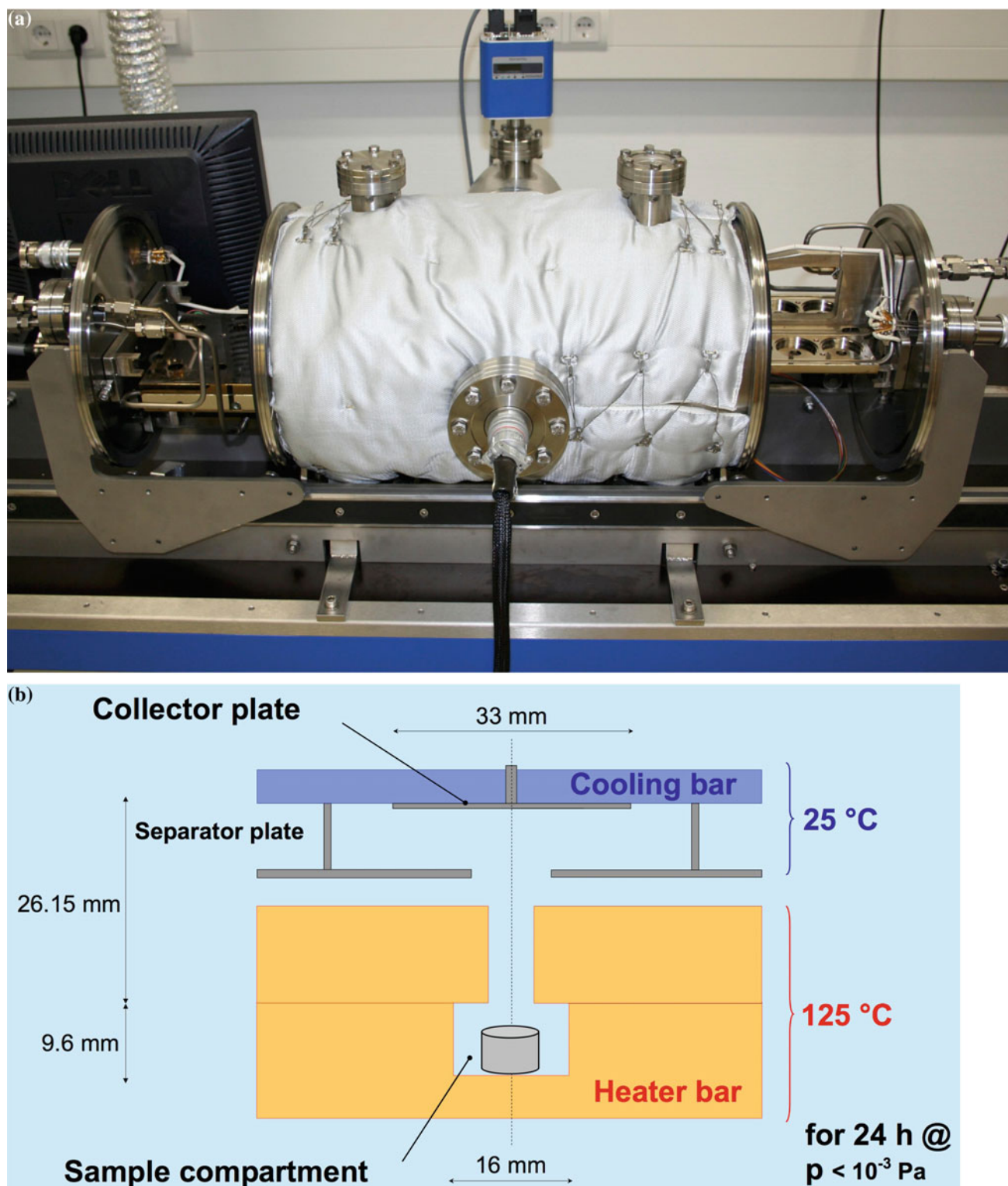


Fig. 2.19 **a** Photograph of a Micro-VCM test equipment for the determination of outgassing properties. **b** Schematic drawing to show the heater bar and location of the plate onto which collected volatile condensable materials (CVCM) will deposit ESA

rendered non-solderable, even with activated solder flux. It is strongly recommended to avoid the following packaging foams and sheets: polyvinyl chloride, Styrofoam, rubber, paper, wool, silk, nylon and some untested polyurethanes. Better long-term storage media, some of which provide for anti-static discharge, would be glass, stainless steel, polyethylene, Dow Ethafoam 220 or similar, and Azote polyolefin foams and Zotek polymer foams from Zotefoams.

Offgassing is associated with the safety of human life and is addressed during the assessment of materials and specific equipment that will be used in a manned environment such as the International Space Station. European standards for offgassing and toxicity were developed in the 80's during the construction of the ESA Spacelab in order to avoid causing harm to both astronauts and to the hardware in these manned compartments. In fact for such projects, as well as the various equipment and experiments that are supplied to the ISS, it is mandatory that all organic materials are tested for offgassing, toxicity, bacterial and fungal growth as well as flammability. The relevant standards include ECSS-Q-ST-70-21 and -70-29 and NASA-STD-6001.

2.5.2 Classes of Non-metallic Materials

The space community has adopted several classes of non-metallic materials. As a brief summary some of the vast number of suitable materials are listed hereunder. However, it must be recognized that every material will require to be tested to ensure it is suitable for a given project application. Some of the products listed are contained in the datasheets annexed to ECSS-Q-ST-70-71.

Optical materials such as organic glasses, oxide ceramics and amorphous inorganic glasses (need to consider radiation environment to avoid damage and “yellowing”): Makrolon (polycarbonate) from Bayer; and Spectrosil fused silica from Optik Heraeus. Zerodur is selected by many companies for the manufacture of space and ground-based telescopes, it is a lithium aluminium silicon oxide glass ceramic characterized by evenly distributed nano-crystals within a glass phase matrix having an extremely low expansion coefficient.

Optical fibres have come into a class of their own and are more frequently selected for box-to-box optical communications within spacecraft. Each fibre, generally made of silica sometimes containing a germanium dopant, is an optical waveguide that can transmit light along its axis. Optical fibres are manufactured as a core inside a clad layer and an outer protective coating. They have advantages over copper electrical wires in that they are lighter, chemically inert, do not corrode and can be easily joined (see also Sect. 6.14). Important for space use, they are immune to electromagnetic interference, and are electrically non-conductive so avoiding short circuits and grounding problems. One drawback is the

radiation induced damage to these fibres—but this will depend on the orbital altitude and proximity to the Van Allen belt. The Long Duration Exposure Facility (LDEF—see Fig. 8.12) demonstrated that after 69 months in LEO no damage ensued except for one cable hit by a micrometeorite.

Adhesives, coatings and ATOX-resistant paints: Araldite AV 138 with hardener epoxy from Huntsman; DC93-500 space grade encapsulant from Dow Corning; RTV 566 silicone from Momentive Performance Materials; MAPSIL 213 silicone potting and MAP ATOX 41-8 varnish for atomic oxidation protection, also electrically conductive brown adhesive QS 0225 EA83, thermally conductive white adhesive QS 1123 TA66 and black general adhesive QS 1123 CEIT, all from MAP Technology.

Adhesive tapes (for flight or temporary use): Scotchtape No. 5 from 3 M Company; Eccoshield PST CA from Emerson and Cummings.

Paints (can be epoxy-, silicone- and polyurethane-based, with or without pigments such as zinc oxide and titanium oxide (white) or carbon black (black)): MAP SG121FD white non-conductive flexible; New paints compliant with REACH, being water-based, and having no ITA restrictions are: AQPUI a non-conductive paint, and AQPUIK a conductive paint; all from MAP Technology; Aeroglaze Z306 black polyurethane with high thermal absorptivity from LORD Corporation.

Lubricants: Dry MoS₂ (alone or within a Teflon or polyimide binder), Fomblin Z25 silicone oil from Solvay Plastics; see also organic lubricants listed in Table 5.2.

Potting compounds, sealants and foams. It should be noted that there is a great variation in the effectiveness of sealants—that is, the time for moisture to permeate various sealant materials. Generally silicones are poor sealants for moisture, epoxies are better followed by fluoro-carbons, but for truly hermetic seals only glasses or metals can be considered: Solithane 113–300 two part urethane from EV Roberts; Stycast 2651-40 dielectric epoxy, and other low outgassing products from Henkel or Emerson and Cuming.

Reinforced plastic composites (usually carbon, glass, Kevlar, Zylon or boron fibres, whiskers or chopped fibres, in a polymer matrix). These are used for both structural and electronic applications: Applications for reinforced plastics can be found throughout this book by making an index search. Fasteners such as bolts, screws and pins give ultimate weight saving choices for applications with moderate loads, with ½ the weight of aluminium and 1/5th the weight of steel—they are resistant to harsh chemicals. With other composite materials they have a matched CTE and superior galvanic corrosion properties while being electrically and magnetically transparent. Various fastener products from Click Bond, Inc.

Rubbers and elastomers. Used for damping systems, clamps, seals and bladders for fluids: Viton B-910 from

DuPont; SIFA-35 and AF-E-332 from PSI Corp. It is essential to know the properties of these materials over a wide range of temperatures as will be highlighted by the explosion, and loss of life, of the space shuttle *Challenger* (STS-51). This accident was caused by a sequence of events, but the engineering cause related to the low temperature mechanical properties of the elastomeric O-ring seals that interfaced the joint between the two cylindrical lengths of each booster. The seals were designed to be compliant between the two metallic joint faces in order to prevent hot gas, under huge pressure, escaping during take-off. The STS-51 launch took place during an unusually cold period at KSC which caused the elastomer to shrink and loose elasticity—this caused the hot combustion gases to escape, burn the seal and release enough gaseous fuel to cause melting of the case and the catastrophic explosion.

Thermoplastics. Often used for multi-layer insulation (MLI), second surface mirrors, electronic wire insulation and sleeving: a multitude of products such as Kapton H, FEP, PTFE are produced by companies such as BASF, ICI and Aventis.

Thermosetting plastics. Usually thermosetting polymers consisting of base, hardener and catalyst which when mixed have a determined shelf life: products include Araldite CT205 as used for printed circuit board lamination; and, Epikote-828.

Obsolescence can be a problem with inorganic materials. Production lines may have ceased due a material's lack of demand. The 'space market' is very small compared to other industries and some costly production processes may cause the manufacture of space-approved products to be unprofitable. For instance, RT/Duroid 5813 was extensively use in the space industry for ball bearing cage applications, but manufacture of this precision bearing material stopped in the mid-90's. Stocks were exhausted just before a replacement material was found—identified as PGM-HT (a composite of PTFE, glass fibre and MoS₂). Although thought to be a direct replacement for Duroid, the PGM-HT was found to shrink on returning to room temperature after heating under vacuum. After much more searching and testing at the European Space Tribology Laboratory (Buttery 2011) another material was found: Sintimid 15M/Tecasint 1391 which is currently considered to be a viable alternative to the recent, US-sourced, Vespel SP-3. Incidentally, the RT/Duroid laminates produced by Rogers Corporation for space electronic printed circuit boards (high-power and microwave) continue to be produced, they consist of PTFE filled with random glass or ceramic micro-fibres.

2.5.3 Novel Non-metallics

- (a) **Vespel** (DuPont) has been utilized more frequently for spacecraft applications during recent years as inferred by the previous paragraph. It is a polyimide-based plastic and has particularly good "space" properties, such as a low outgassing under vacuum, even at high temperatures. The basic material (SP-1) has a low wear rate and low coefficient of friction in vacuum and moisture-free environments. The tribological properties of Vespel can be further enhanced by the additions of 15 % graphite (SP-21), 10 % PTFE (SP-211) or 15 % molybdenum disulphide (SP-3). The low thermal expansion of all Vespel variants are between 35 (SP-21) and 55 (SP-211) ppm/°C, relatively low for polymers (when compared to values listed in Appendices 1C and 1E). Vespel has been used in a spacecraft's liquid helium cryostat, as a valve seat, selected for its stability at cryogenic temperatures (see Fig. 5.71). As an example of its versatile temperature use, Vespel has also been demonstrated as a successful non-metallic interface material against aluminium in the design of the electric propulsion pointing hold down and release mechanism of Bepi, qualified from −40 to +150 °C under contact loads of between 15 and 60 MPa (Janu et al. 2009).
- (b) **Graphine.** This is the thinnest compound known to man and comprises of a thin layer of pure carbon. The carbon atoms are bonded together in the form of a hexagonal, honeycomb lattice. It is a two-dimensional carbon monolayer and being only one atom in thickness, it is the lightest material known to man (1 m² weighs about 0.77 mg). Graphine is also the most electrically conductive material available and although it has the potential to be used for spacecraft communication equipment, with vast weight savings, it can only be produced in very small sizes and quantities. Applications include durable display screens, electrical circuits and solar cells. Graphine is produced by chemical vapour deposition (CVD) and this process deposits carbon in the form of multi-crystals having a single-layer sheet of carbon atoms. It is these grain boundaries that are thought to affect the larger-scale properties of the sheet, such as thermal and electrical conductivity. The grain orientations and surface topology of graphine has been observed by atomic-resolution transmission microscopy (Chuvilin et al. 2014). Possibly graphine could also be used to

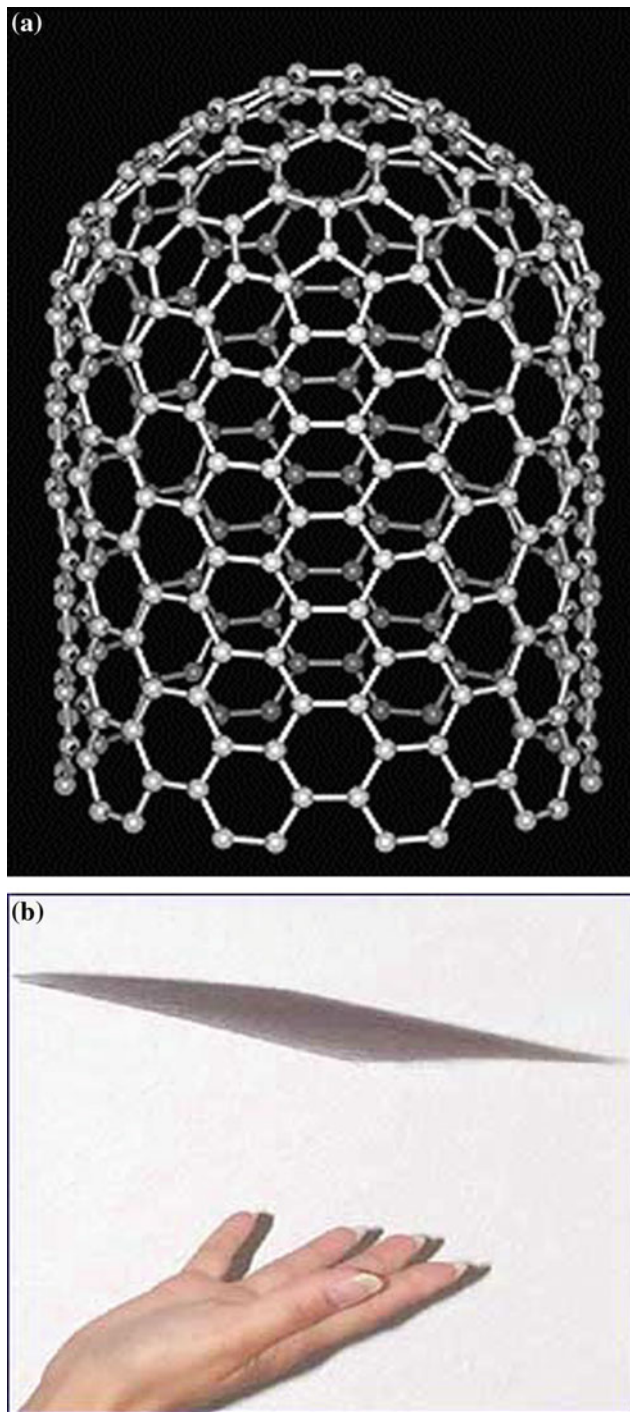


Fig. 2.20 **a** Depiction of the carbon nanotube structure; properties can be used to create the strongest known fibres, they can be very flexible and foldable. **b** Illustration of an ultra-low density inorganic foil which can be made from carbon fibre mesh, open-cell SMP foams and aerogels. Once unfurled, they are stable, moderately heat-resistant and could be used for solar sailing. They could overcome current deployment limitations by being self-deployable and very large structures can be envisaged (Dunn 2001)

build a large solar sail; it would have the smallest mass per unit area and, if the material could be manufactured into large sheets, it could sail using solar radiation (photons) from the Sun. By adjustment of the sail's angle relative to the Sun, the sail could be steered so as to tack towards or away from the Sun and could progress to the edge of the Solar System. To date, only beryllium sails have been considered possible as they can be produced to a thickness of about 40 nm. Plastic thin films are likely to vaporize once they are unfurled and exposed to ultraviolet radiation. Similarly, the high-energy, ionizing solar photons may degrade and make the properties of the graphene sail unobtainable (Matloff 2013).

- (c) **Carbon nanotubes (CNT)** are, like graphene, a great challenge to engineers who are attempting to utilize these cylindrical rolls of carbon molecules (Fig. 2.20a). As CNTs have a density 50 % less than aluminium and a tensile strength of 10–60 GPa (an order of magnitude greater than the strongest steel, or Kevlar) the material could be formed into a composite for highly efficient space structural applications. Carbon nanotube based composites and carbon-carbon are currently under study as structural materials for space telescopes, optical benches and large mirrors. CNTs may have tuneable electronic properties from metalloid to semi-conductors.
- (d) **Graphite fibres** having a thermal conductivity of over 800 W/m-K, are now being bundled with a polyester cord to form Thermal Straps that can be used as flexible thermal links (or heat straps). The US company, Technology Applications Inc. is the only producer of these fascinating straps. They are extremely light, flexible and up to one tenth the weight of equivalent copper straps. These Thermal Straps have been used as heat pipes in spacecraft applications where extremely low outgassing is required. They have a variety of end fittings; aluminium and copper can be selected to avoid galvanic couples or corrosion.
- (e) **Shape memory polymers** or so-called SMPs (as opposed to SMAs, the alloys described in Chap. 4.18) are only recently being considered for industrial applications; these are based on covalently cross-linked polymers, and their shapes can be changed by the application of heat and electric fields. Damage to spacecraft antennae or structures caused by space debris may be mended and accurate profiles restored by realigning those surfaces to face solar radiation from the Sun (Athimoolam 2012). These novel, and gossamer-like materials may also be used as ultra-light materials for self-deploying structures as shown in Figs. 2.20 and 2.21.

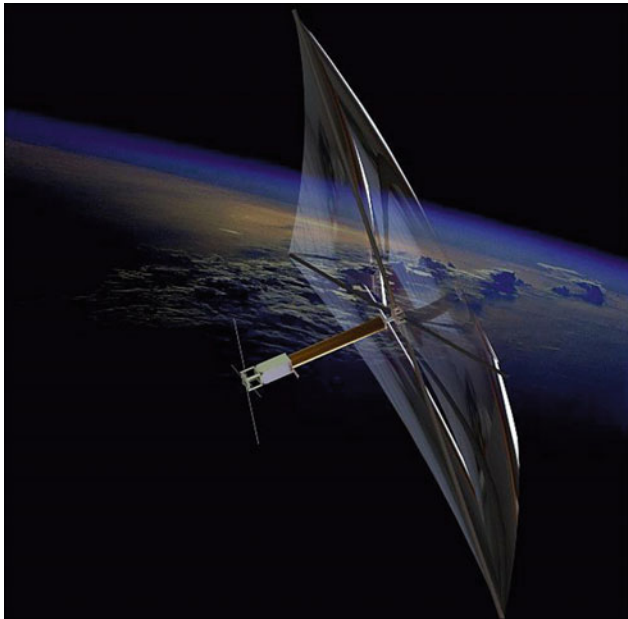


Fig. 2.21 Illustration of the InflateSail 3U CubeSat with 1 m long inflatable boom and 10 m² deorbiting sail proposed by Surrey Space Centre at the University of Surrey. The primary goal of this concept project is to attach such a sail to a low Earth orbiting satellite at the end of its life and use the sail to remove it from orbit (*image credit SSC*)

Many other new materials are under investigation for space use. *Arall*^R is a fibre-metal laminate having aramid fibre-prepreg sandwiched between sheets of aluminium alloy. *Glare*^R consists of aluminium alloy sheets bonded by glass fibre prepreg. Metal matrix composites and ceramic matrix composites will be referred to in subsequent chapters.

- (f) So-called **self-healing materials** have been considered for the repair of military vehicles and battle jackets, ships and airplanes during the past twenty years. They have also been studied for spacecraft applications (Semprimoschnig 2007). Probably the most promising system is based on fragile microcapsules. These can be incorporated into an organic coating and, for instance, when the coating is damaged due to impact or fatigue cracking, the microcapsules in the proximity of the defect will break and release a mix of polymerizing liquids that then cure and heal the damaged area. A similar concept, but based on hollow fibres (see Fig. 2.22), has been developed by the University of Bristol where healing occurs when an epoxy resin-solvent is released from the fibres and flows onto a complex catalyst contained within the matrix and is exposed at a crack front (Coope et al. 2014). Clearly, self-healing materials are of great interest for space missions where there are threats from impacts by micro-meteoroids and space debris; remoteness and the

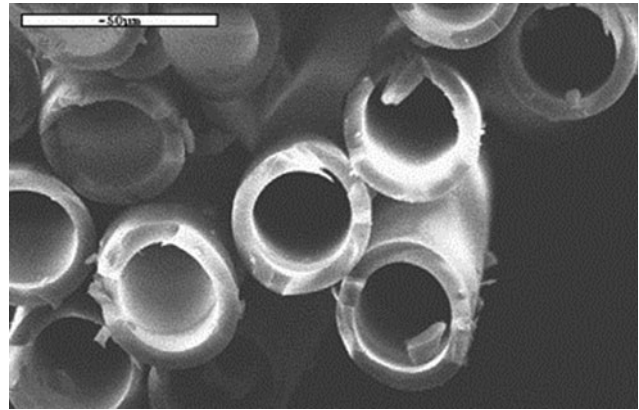


Fig. 2.22 Example of an early “hollow fibre repair” sample seen by electron microscopy. The release of the repair agents from within these storage reservoirs mimics the bleeding mechanism in living creatures. Here, alternate hollow fibres contained a resin and a hardener. Work by Dry, C. reproduced for the STFC Workshop (Semprimoschnig and Eesbeek 2007)

inability to make effective repairs in space will spur on further developments in this discipline of materials science.

More often scientists and materials engineers are looking to nature for ideas as how to “make structures stronger to improve their performance or lighter so that they use less material”—these aims have been expounded by Professor Barber’s team at the University of Portsmouth in their study of limpet teeth (Barber et al. 2015). These small teeth were found to be composed of a composite structure containing **goethite nanofibers**, $\alpha\text{-FeO(OH)}$, distributed within a softer matrix of a protein phase. The tensile strength of miniature dog-bone samples, removed from the limpet teeth by cutting with a focused ion beam in vacuum, was found to range from 3.0 to 6.5 GPa. Each sample was “milled” using a focused ion beam attachment to a scanning electron microscope and the results can be seen in Fig. 2.23. The strain behavior at fracture being between 4 and 8 %. These values are equivalent to the strongest man-made fibres such as Toray T1000G carbon fibres with a tensile strength of 6.5 GPa.

- (g) Another interesting development is the in-laboratory manufacture of **Gecko biomimetic adhesive tape** for space applications such as holding down Multi-Layer Insulations (MLI) and other reflective or protective films. Microscopy has determined that a gecko’s foot has about five hundred thousand keratinous hairs, each up to 130 μm in length and having a diameter of one-tenth that of a human hair. The first direct measurements of a single hair’s adhesion property was made using a two-dimensional micro-electro-mechanical systems force sensor (Autumn et al. 2000). The adhesive forces of

the hairs were thought to be governed by the ultra-efficient application of van der Waals forces. The mimicking of gecko hair properties has been attempted in a large Italian study (Gregoratti et al. 2013). Vertically aligned multiwall carbon nanotubes (VA-CNTs) were grown on both rigid and flexible metal substrates using lithographic techniques: some gecko adhesive properties were achieved but it seems more questions than answers are recorded at this early stage in the study (Gregoratti et al. 2013): How do the gecko properties respond to changes in temperature and humidity? What is their long-term reliability in specific environments? Can such a material surface be made robust and reliable? And, most importantly, can they ever be fabricated cost-effectively over large areas?

- (h) Although not entirely a new material to the space materials engineer, **cork** is finding more interesting and novel applications. Owing to the chemical and physical structure of cork—the natural bark growing on the trunks of cork oak trees (*quercus suber*)—this material has found important uses as ablative material on re-entry vehicles. As listed in Table 2.7, cork has a low density and low thermal conductivity. Cork—called nature’s foam by NASA—is 90 % gas and is essentially a structure made up of dead cells, each having a polyhedron of only 30–40 μm in diameter (Coelho 2009). Ablative materials protect space vehicles from the severe aerodynamic heating during launch and during re-entry into the atmosphere at velocities greater than 7 km/s.

The ablative materials used on the re-entry capsules of first US manned missions, Mercury, Gemini and Apollo, were based on cork. It was used on the solid rocket boosters of the Shuttle and applied to the booster nose-cone and frustum of Delta launch vehicles. In Europe, cork-based ablative materials were applied to the front and back covers of Beagle-2, are used on Ariane-5, the Atmospheric re-entry demonstrator and Mars Express (Bouilly et al. 2006, 2013). Illustrations of cork being applied to space hardware are shown in Figs. 2.24 and 2.25.

Cork is fire resistant and chars rather than burns. As a thermal protection system (TPS) it undergoes several physiochemical changes each of which are heat-absorbing. Initially it heats up, then the front exposed surface is thermally degraded (charred), gasses released during pyrolysis pass through the charred layer which becomes thicker. Gas reaction with the carbonaceous layer creates channels through which gas and reaction products are released as ablation vapours. This releases thermal energy into the air flowing past the structure. The cork composite is formulated so that as it chars, the interface between the advancing char and the underlying (virgin) material causes chemical reactions

that are either exothermic (at the lower temperatures) or endothermic (as the material sublimates). The charred layer is a good insulator, it has a good emissivity and, as its surface is eroded in the flow of passing air, further heat is dissipated away from the structure. Extensive studies into chemical reaction, ablation mechanism and morphology of the resultant black charred layer include those of Asma et al. (2010). A recent EU-funded project called Aerofast has provided promising results for two new families of TPS materials fabricated from cork supplied by Norcoat-Liege and Amorium Cork Composite (ACC). The work (Pinaud et al. 2014) also validated a 3D charring ablation model taking into account the decomposition of the TPS at various temperatures, its decrease in thickness and required dimensions for various aerodynamical shapes.

The protective cover attached to US spacecraft bound for Mars is called an “Aeroshell”. The Aeroshell is constructed from an aluminium honeycomb, covered with graphite-epoxy face-skins that are in turn covered with a phenolic honeycomb containing ablative material. The ablator is a unique mixture of specially graded cork granules, binder and silica glass microspheres. The chemical formulation of this mix is designed so that as the probe or landing craft enters the Martian atmosphere, friction causes the ablator to undergo chemical reactions and char. This has the effect of dissipating heat which is “taken away” by the hot wake of gas behind the vehicle. Thermal protection system must be able to resist temperatures which could reach 1600 °C during entry into the Martian atmosphere, and yet maintain a temperature of less than 125 °C inside the probe. The tiles can be formed and individually machined on all six faces, then bonded to the probe surfaces with silicone blue, ESP 495.

- (i) A material finding many new applications is **expanded polytetrafluoroethylene (ePTFE)**. The microstructure mimics some cell structures found in nature, as seen in Fig. 2.26. The main usage of ePTFE in space applications is as a low dielectric constant (1.3) insulation material for high-speed digital coax cables. Here, ePTFE provides high signal quality and optimum performance in miniaturized systems where conductor sizes as small as AWG 42 can be manufactured. As this material is inherently inert, thermally resistant and hydrophobic, it can also be processed into high-flowrate microporous membranes. Applications will be as filters within manned spacecraft modules for air and potable water purification systems. ePTFE filaments have recently been incorporated into a fibre-reinforced matrix (such as PEEK) as a reservoir for solid lubricants. The porosity of ePTFE, as seen in Fig. 2.26, can be processed to vary from 5 to 90 %.

Fig. 2.23 Scanning electron micrographs showing (a) the limpet tooth prior to FIB milling, and (b) milling to thin the sample towards a “dog bone tensile sample” geometry (c) shows plots of stress-strain for individual limpet samples with a variety of lengths that were tested to failure using an atomic force microscope (Barber 2015)

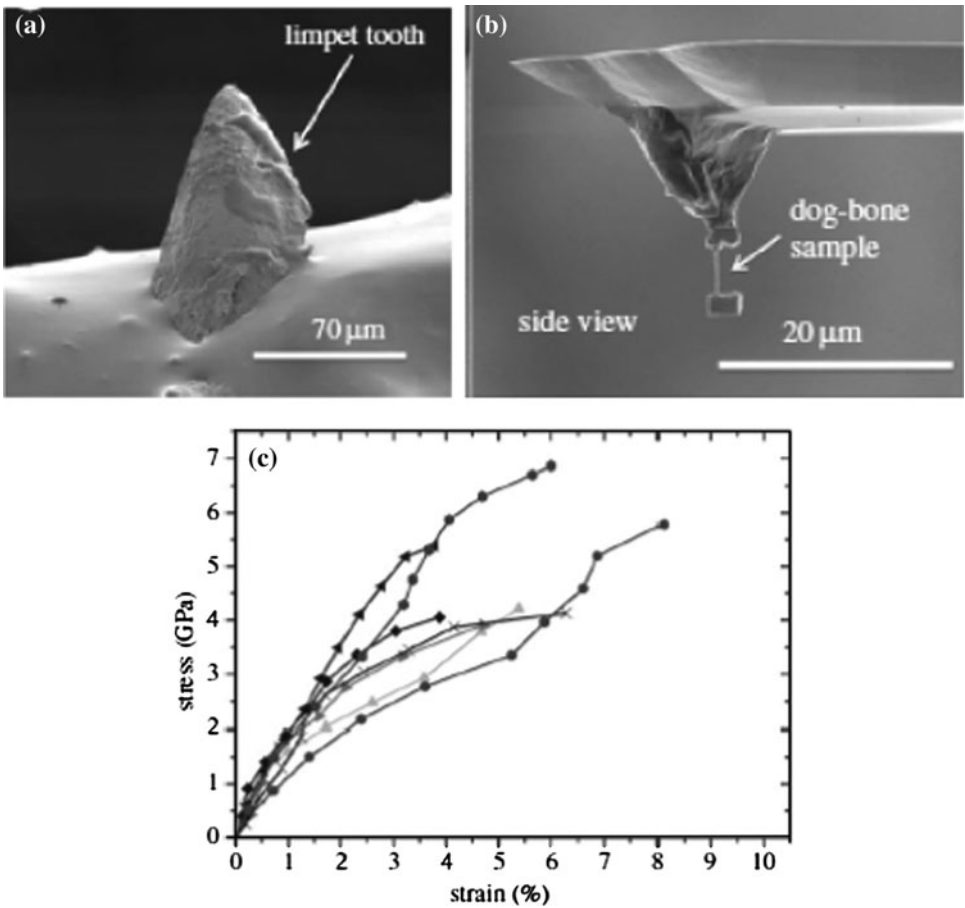


Table 2.7 Three varieties of thermal protection systems—their sizes and properties (by permission of Amorim Cork Composites ACC, Mozelos VFR, Portugal)

	P45	P50	P60
Cork particle size (mm)	1–2	0.5–1	0.5–1
Sheet dimension (mm)	1270 × 710	1270 × 710	1000 × 500
Sheet dimension (in)	50 × 28	50 × 28	40 × 20
Density @ 20 °C ^a	0.32	0.48	0.45
Tensile strength (psi) ^b	110	250	160
Tensile strength (MPa) ^b	0.76	1.50	1.10
Elongation (%) ^b	30	13	7
Thermal conductivity (Btu in)/(h ft ² °F) ^c	0.45	0.50	0.55
Thermal conductivity (W)/(mK) ^c	0.06	0.07	0.08
Specific heat (Btu/lb °F)	0.6	0.5	0.4
Specific heat (KJ/Kg/K) ^d	2.5	2.1	1.9
Substrates to bond		Metals and composites	

^aASTM F1315

^bASTM F152, method B

^cASTM C177

^dASTM C351

Work by the University of Florida (Vail et al. 2011) is on-going: to regulate wear in tribological applications by the secretion of very thin lubricant films from the

pores of the included ePTFE filaments onto the contacting surfaces of mechanisms. As all materials under evaluation appear to be stable in a vacuum/space



Fig. 2.24 The Beagle 2 Mars entry probe fitted with cork TPS. **a** Front-shield and back cover inspection in assembly workshop. **b** Front-shield tile being bonded—prior to packing in bio bags and sterilization treatment

environment, such novel lubrication methods might eventually be applied to spacecraft mechanisms.

- (j) **Liquid crystal polymers (LCPs)** have been evaluated by NASA Glen and are said to out-perform conventional polymeric materials for application as flexible printed circuit substrates and large flex-antenna arrays that can be rolled into cylindrical shape and launched into space (Kingsley 2008). These LCPs are heat resistant, strong and light-weight—ideal properties for space applications. LCPs have been commercially available for two decades, but modern process have enhanced their strength and ability to be formed into exceedingly thin sheet and fine wires. The wires have been compared to spider’s silk, being of exceptional strength, and “comparable to steel-wire”. LCP sheet can be made to melt at 290 °C or 315 °C, at the lower temperature it is called bondply and at the higher temperature, the core. So, by utilizing bondply between two cores, and applying heat to slightly above 290 °C, an inseparable bond is achieved. Multiple stacking can be made, rather like a flexible multilayer board, with metal vias, printed interlays of metal, and even embedded

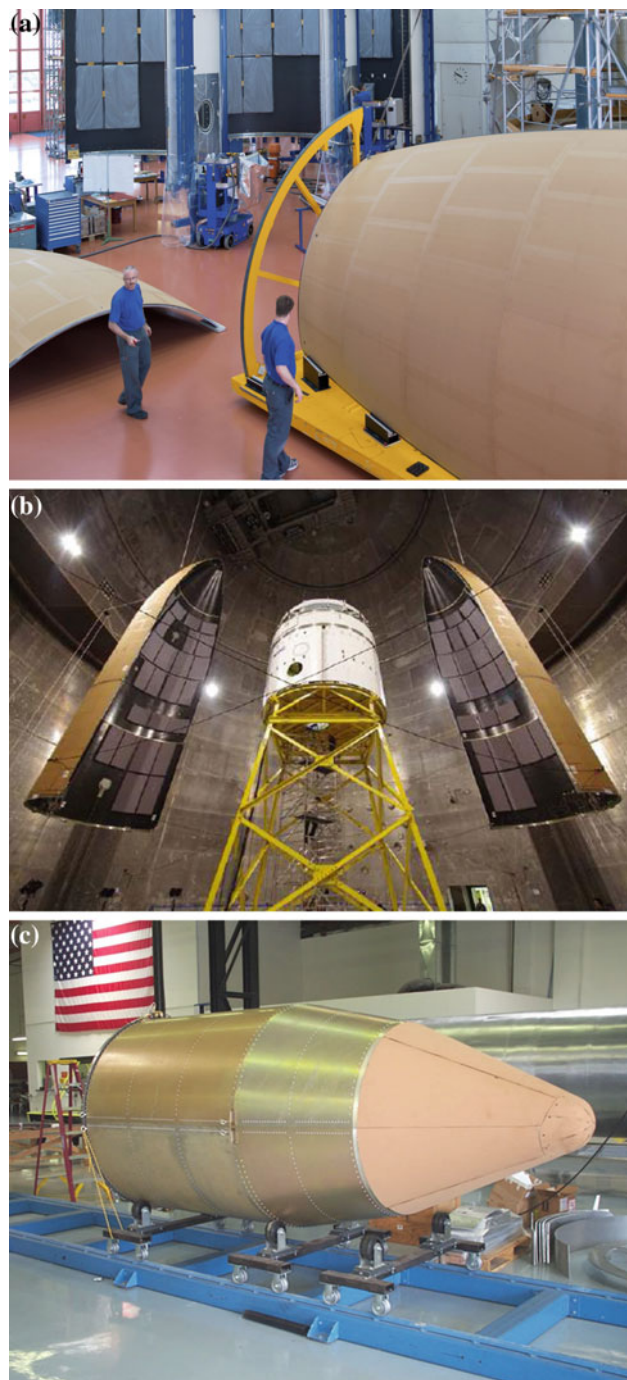


Fig. 2.25 **a–c** Cork is applied as a TPS onto fairings and nose cones of modern launch vehicles such as Ariane 5, Vega and the SpaceX Falcon. Its long heritage includes successful use on Atlas V, the former Space Shuttles and Apollo missions

components. The material can be made with a thickness of 25 μm , it has a low water absorption of up to 0.04 % (but is permeable to water) and resists degradation due to radiation in space. The Japan Aerospace Exploration Agency (JAXA) has used very thin LCP sheet material for solar sail applications, several have been successful.

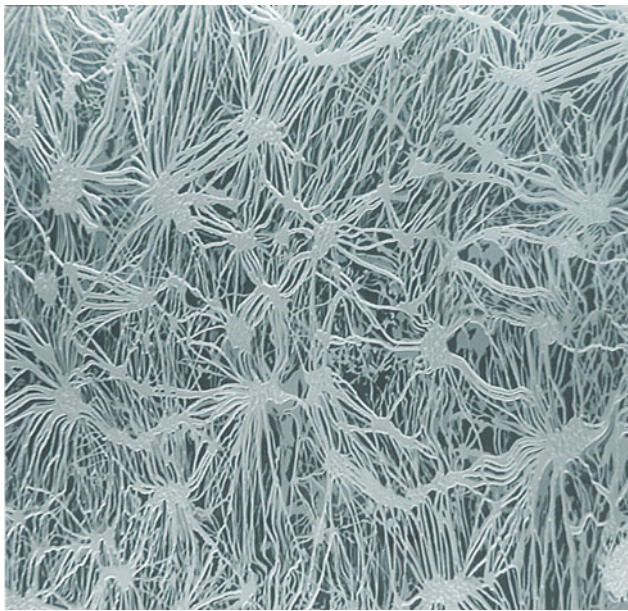


Fig. 2.26 Electron microscope image of expanded PTFE membrane. This is seen as a fibrillated form of PTFE; with a porous network of fibrils connected to dense nodes of PTFE. Magnification of 40,000 times

One named Ikaros recently passed Venus and JAXA are now considering future sail missions, powered only by the Sun's light particles, to Jupiter and the asteroid belt.

Returning to LCP wire, Vectran™ is said to be the only commercially available melt-spun LCP fibre in the world; weight-for-weight this fibre is five times stronger than steel, has a high abrasion resistance, cut resistance and has good mechanical property stability over a wide range of temperatures. These fibres can be coated with copper, nickel or silver and is available (Liberator™ Conductive Fiber) in bundles comprising of 20, 40 and 80 individual filaments. This is a new product and has been used as a woven braid material for cables. The new braid material will be of interest to spacecraft harness fabricators due to its substantial weight savings over copper braid as illustrated in Fig. 2.27.

2.6 The Potential for Welding and Joining in a Space Environment

2.6.1 Background Considerations

Large dimensions and mass mean that structures such as the International Space Station (ISS) cannot be transported as one complete structure into low Earth orbit. They must be launched in sections and assembled in space (and as already

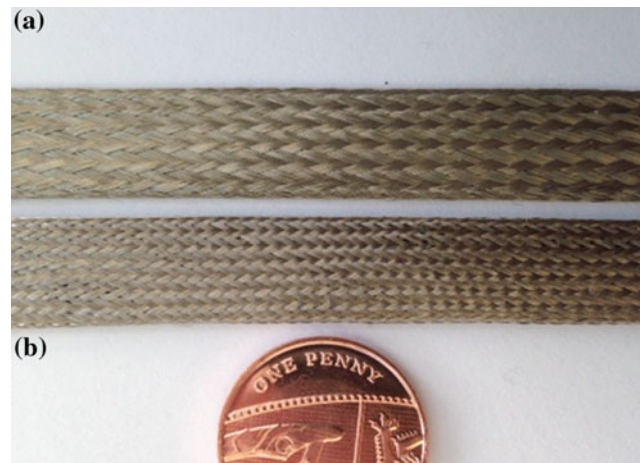


Fig. 2.27 Braided sleeves, each 11 mm wide, for coaxial cables (a) is standard nickel-plated copper braid, (b) is a novel braided sleeve utilizing Liberator™ nickel-clad conductive LCP fibres. These novel fibres are 15 times stronger than copper and 86 % lighter; for a RG142 coax cable the overall cable is 40 % lighter than a standard shielded cable

discussed, in future missions assembly may occur on the surface of our Moon and possibly other planets). So far, little work has been specifically dedicated to intra-vehicular and extravehicular activity (IVA and EVA) joining and cutting issues in space. This section will revisit some of the findings of Dunkerton et al. (2001) and include more recent welding developments having relevance to space applications. By far the largest contributions made to date, on the development of welding and brazing technologies for use in space (Dzhambekov et al. 1991; Paton 2003), have been made by Russia:

1969—Vulkan, for electron beam (EB), low-pressure plasma and consumable electrode welding
 1979—Ispartel, the depositing of thin coatings by condensation and evaporation
 1983—Ispartel M, deposition of braze metals
 1984—development of a versatile hand-held tool for cutting, brazing, welding, heating and coating
 1988—Yantar—EB coating and welding
 1990—Universal Hand-held 3 kW manual EB gun used on Mir Space Station. (Figs. 2.28 and 8.33)

Reference to the numerous metallurgical experiments performed in the space environment by astronauts and cosmonauts, for instance on Skylab, Soyuz, Mir and the Salyut spacecraft, have been compiled by Flom (2005) and by Paton in his reference book (2003). The majority concerned the melting and joining of metals in space. Flom (2005, 2006) noted that the vacuum of space is higher than a typical Earth-situated vacuum chamber can provide so that electron beam welding would require very little power and cathode

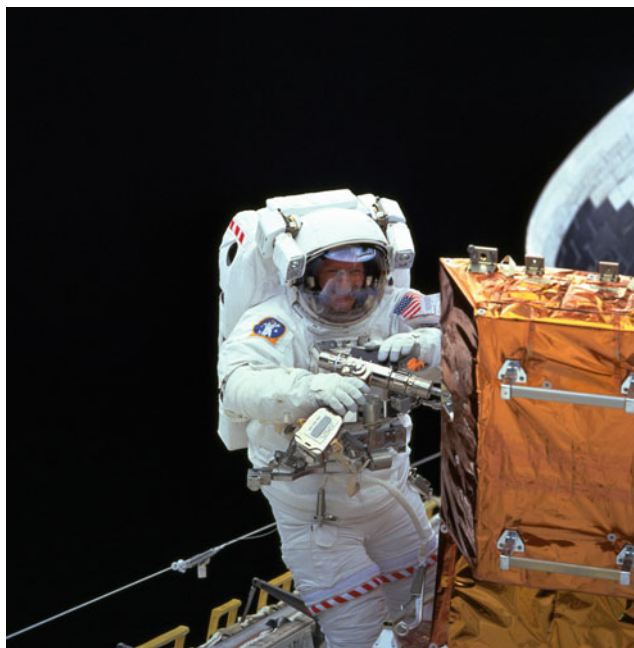


Fig. 2.28 ESA astronaut Claude Nicollier at work in December 1999 making repairs to the Hubble Space Telescope with a mechanical fastener tool during the refurbishment mission (courtesy NASA)

life would be enhanced; he further describes the NASA GSFC study for electron beam brazing. These were not pursued during the construction of the ISS which is based on modular assembly; the interconnection of its units uses rather traditional mechanical joints designed to be compatible with EVA astronauts. For instance, truss joints are assembled by using tubular parts that are interlocked by first insertion, twisting and locking. Mechanical fastener tools have been used for more than two decades, one operation is shown in Fig. 2.28.

The use of mechanically assembled trusses for assembling large structures is described by Watson et al. (2002), but in a later NASA work (Dorsey et al. 2012) proposes that although astronauts and robots can efficiently construct space structures with mechanical connections, it is the use of custom-built welded structures that will be the game-changers of the future.

The majority of spacecraft materials are coated (e.g. inorganic paints, silicones, specially conducting indium tin oxides, alumina, silica, platinum, gold, and chemical conversion coatings such as Alodine and the anodisation of aluminium alloys). This provides protection from terrestrial corrosion prior to launch. Coatings are also designed to ensure that surfaces have stable features, such as adequate resistance to atomic oxygen and constant solar absorption and emission properties in orbit. These coatings may affect subsequent joining/cutting operations. Therefore there is a

certain antithesis between coating of the structure to ensure its stability and resistance to degradation, whilst still ensuring that the joining/cutting process is viable.

If one considers using welding or other processes for repairing manned habitats it is essential that the Whittle “shields” (to protect habitats from micrometeorites and man-made debris as described in Sect. 8.4.4) are removed in order to access the module’s wall. Shields and thermal blankets if not detachable, can form a physical barrier to EVA joining/cutting activities in terms of accessibility and/or temperature constraints.

If joining techniques are to be applied for construction activities in space it will be important to consider the following list of critical factors:

- Range of material compositions, their coatings and form, including thickness
- Portability/ease of use/stability of the tool under vacuum (e.g. lubrication)
- Health and safety
- Energy requirements
- Surface preparation/fit-up/jigging
- Metallurgical implications and joint performance
- Processing debris must be avoided
- Intra or extra vehicular process application
- Equipment maintenance
- Gravity effects
- Joint hermeticity.

2.6.2 Potential Joining and Cutting Processes

The following “non-mechanical” processes can be considered:

Adhesives, Arc welding, Brazing, Electron beam welding, Friction welding and Laser welding.

These processes can be considered against the criteria listed in Sect. 2.5.1, to select the most promising techniques as noted below. However, it must be noted that these considerations are subjective and would need extensive further evaluation:

Organic Adhesives

These offer a nominally simple means of bonding two materials together, with fairly simple equipment and at reasonable cost. They might be the most suitable means for joining carbon fibre reinforced plastic components that have been designed to incorporate lap-joints into which adhesive resin can be injected. However, adhesives are not considered to be suitable for general application during IVA or EVA activities since such joints suffer from poor hermeticity, usually high outgassing rates prior to curing under vacuum and unknown reliability over time.

Arc Processes

The fundamental argument against using arc fusion processes in space is that an ionised gas, or plasma, is required for any of the processes to operate. This means that, generally, arc processes exhibit a lack of vacuum stability and require copious amounts of gas. Gas is supplied either from pressurised gas cylinders, or by a flux coating. However, a variant of gas tungsten arc welding (GTAW) However, a variant of the GTAW process, which uses a hollow tungsten electrode, was first developed for welding in a vacuum during research activity starting in 1965 at the E O Paton Electric Welding Institute. This equipment was tested in October 1969 on the Soyuz 6 spacecraft (Fig. x) but the process did not fulfil expectations. GHTAW (gas hollow tungsten arc welding) requires only 1/100–1/1000 the flow rate of gas normally used at atmospheric pressure, but even this concentration of plasma-forming gas in the arc gap zone could not be maintained. Development work continued and in 1973 Shiganov (1973) reports that a highly stable arc discharge could be maintained in an evacuated chamber on Earth. In 1986, Rocketdyne, a division of Rockwell International, began development of similar hollow electrode technology in the US. In 1989, Rocketdyne prepared a report for NASA proposing an extravehicular activity welding experiment and trials, made in drop-shafts and in low gravity aboard an aircraft, gave encouraging results (Watson and Schnittgrund 1989).

The GTAW process offers the following advantages: Operation in both the vacuum environment in space and the pressurised environment inside the space vehicle is possible. Relatively wide tolerance in process variables (travel speed, position and arc length) enables manual operation. This process is easily automated and relatively safe.

GTAW is widely used to weld all common aerospace alloys—e.g. steels, Al and Ti alloys and is an established technology.

However, there are a number of notable disadvantages to this process, namely: a gas supply required (heavy cylinders, need refilling or replacing); is not a cutting technology. Electrode damage due to vaporisation in vacuo (need to regrind or replace) and vaporised products may condense and contaminate astronauts' visor and other critical surfaces. Also, electromagnetic interference (EMI) may interfere with electronics systems, plus high voltage or HF surges on arc initiation could draw power away from other systems.

Therefore, it is considered that, whilst a useful technique, there may be other welding methods of greater merit.

Brazing

Brazing is of limited use for the assembly of large structures in space, especially if they are made from alloys such as AA2219, due to the lack of suitable brazing alloys. The removal of oxidation layers (from ground storage) or protective coatings would be required prior to any brazing operation. Presently the most suitable/versatile method for the heating of braze alloys is via an electron beam. This technique is difficult to adapt for the repair/patching of damaged structures. Flom (2006) has, however developed a low temperature brazing process, where heat is delivered from an electron gun and, under high vacuum, braze alloys based on Au-Sn can easily be drawn by capillary action into specially pre-prepared joints. [Flon's EB brazing process was used in the refurbishment of an Italian spacecraft electrode housing, see Sect. 4.28].

Electron Beam Welding

Electron beam welding is particularly suitable for use in space. EB can be used as a very controllable heat source for welding, brazing, soldering, cutting, original manufacture, repair etc. on electrically conductive substrates. The material heated during the welding process is minimal—limited to a very narrow fusion zone (of say 1 mm for a joint of 3 mm thickness) and the heat affected zone (extending say 0.3 mm beyond the fusion zone). As little material is heated, the process is extremely efficient compared with arc welding techniques. The method is utilised throughout the space industry for the fabrication of space hardware, as described in Sects. 4.2 and 4.13. Although narrow welds may be produced with some lasers, the efficiency of electron beam generation can be in excess of 95 % compared with typically 10 % for the most efficient laser. The Russian hand-held low accelerating voltage (<8 kV) electron beam gun (named the Universal Hand Tool)—as described by Paton (2003) and illustrated in Fig. 2.29—has already been demonstrated in space EVAs for EB welding, heating and cutting.

There are two main potential problems associated with EB equipment. First, the process generates X-rays at the point of impingement of the beam on the substrate. By choosing a low ~10 kV voltage, as for the Universal Hand Tool, the additional contribution to radiation exposure during EVA is likely to be small. Secondly, if the welding beam should impinge on (say) an astronaut during EVA, the risk of perforating the spacesuit is significant. In the past this risk was deemed unacceptable by NASA, but recent US activities (Flom 2006, Dorsey et al. 2012) indicate that safety considerations are now acceptable, particularly when it is robots that perform the handling, manipulation and EB welding tasks.



Fig. 2.29 Universal hand-held 3 kW manual EB gun used on Mir space station (*source* from 1999, *Avtomaticheskaya Svarka*, 10)

The EB processes and EB equipment which can be utilised in space are by no means perfect for every application, but they currently offer the best compromise for many applications as well as significant scope for further refinement and diversification in the future.

Friction Welding

Unlike some processes, there is no published data on friction welding in space. The principle of the friction stir welding (FSW) process is described in Sect. 4.25 and characterised by Fig. 2.30. This process is used extensively during the manufacture of spacecraft hardware in many countries. Briefly, the heat is generated by a rotating tool, which consists of a shoulder, which rests on the surface of the material to be welded, and a pin, which penetrates almost the complete thickness. Frictional heat causes material to soften, and the forward translation of the rotating tool causes material to be pumped from the front of the tool to the rear, where it is consolidated under pressure to form a solid state weld. It is emphasised that there is no fusion in this process.

Modifications to the FSW process are termed friction taper plug and stud welding, these have also been adapted to

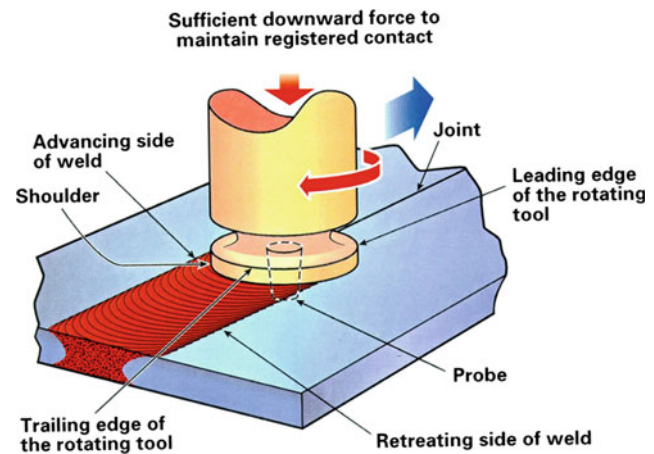


Fig. 2.30 Schematic drawing of friction stir welding

fill holes. There are several distinct processes, in which the process mechanisms differ fundamentally. All of the processes work better on fully penetrating holes, as it is often difficult to completely eliminate defects at the bottom of blind holes. Perhaps the most important process is friction taper plug welding, where a tapered plug is friction welded into a tapered hole. The process has been scaled up to make plugs in material of up to 38 mm, but clearly the equipment becomes more robust and heavier, and the power demands greater. However, for aluminium materials of 10 mm or less, such as the AA2219 alloy plate used on Spacelab and ISS, it is feasible to consider this process.

Friction stud welding equipment is generally light and easily transportable, and the intermittent use of the equipment suggests that overheating of the motor in vacuum is not a major issue. Although it is only capable of welding studs to other structures, this can be developed with a little imagination to enable many construction and possible repair tasks to be undertaken. It is probable that stud diameters should be restricted to about 5 mm in order to reduce mass, and increase ease of use in space, but this will also require an increase in the rotation speed of the motor. Friction stud welding might be envisaged to 'plug' damage caused from micro-meteoroid impacts on pressurised spacecraft as illustrated in Fig. 2.31. Threaded studs might also be attached to space structures and enable the further integration of hardware by mechanical screw fastening in space. Similar EVA was performed by an ESA astronaut (Fig. 2.28).

Laser Welding

Lasers are a very attractive tool for application in space due to their versatility to weld, cut and repair metals and to a certain extent, non-metals. Diode lasers appear to be the most promising candidates due to their high efficiency, small size and low maintenance requirements. However, the

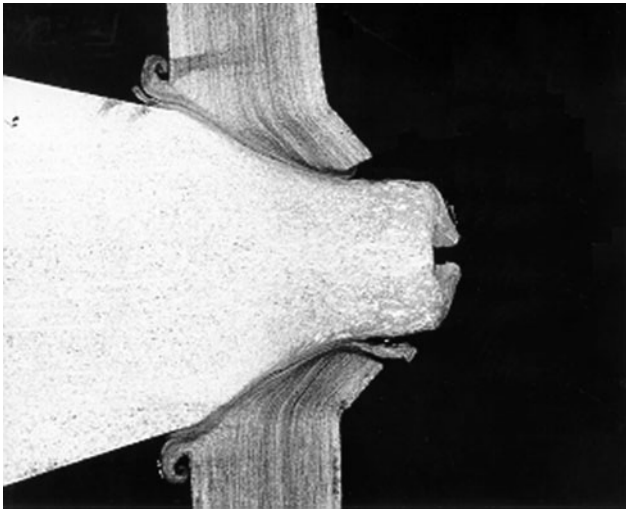


Fig. 2.31 Microsection of friction stud weld made to 3 mm thick plate that contained a simulated impact crater. Note that no material debris was released and a proper metallurgical joint exists between stud and plate (Dunn unpublished)

current developments of diode lasers are not sufficient in terms of power density, to produce welds or cuts within the range of materials and thickness used in space applications.

Nevertheless, it is expected that developments in the brightness of diode lasers will increase the available power density to be suitable for welding and repairing the materials of interest for space applications.

2.6.3 Expectations

1. Electron beam (EB) welding is considered today, to be the most applicable process for both joining and cutting operations. In particular is the ease with which the process can be adapted and its ability to be operated in a safe manner. Extensive work has already been carried out on EB welding in space and suitable, commercially available equipment is already on sale.
2. Friction welding has much potential for use in a space environments, although it is more suited to joining than to cutting. It is a versatile process, which can be used in arduous environments and suitable for the types of materials used in space construction.

<http://www.springer.com/978-3-319-23361-1>

Materials and Processes
for Spacecraft and High Reliability Applications

Dunn, B.

2016, XX, 667 p. 490 illus., 295 illus. in color.,

Hardcover

ISBN: 978-3-319-23361-1